

A close relative of the Amazon river dolphin in marine deposits: A new Iniidae from the late Miocene of Angola (#25005)

1

First submission

Editor guidance

Please submit by **2 Apr 2018** for the benefit of the authors (and your \$200 publishing discount).



Structure and Criteria

Please read the 'Structure and Criteria' page for general guidance.



Custom checks

Make sure you include the custom checks shown below, in your review.



Raw data check

Review the raw data. Download from the [materials page](#).



Image check

Check that figures and images have not been inappropriately manipulated.

Privacy reminder: If uploading an annotated PDF, remove identifiable information to remain anonymous.

Files

Download and review all files from the [materials page](#).

13 Figure file(s)

2 Table file(s)

3 Other file(s)

! Custom checks

New species checks



Have you checked our [new species policies](#)?



Do you agree that it is a new species?




Is it correctly described e.g. meets ICZN standard?



Structure your review

The review form is divided into 5 sections.
Please consider these when composing your review:

1. BASIC REPORTING
2. EXPERIMENTAL DESIGN
3. VALIDITY OF THE FINDINGS
4. General comments
5. Confidential notes to the editor






 You can also annotate this PDF and upload it as part of your review

When ready [submit online](#).





Editorial Criteria

Use these criteria points to structure your review. The full detailed editorial criteria is on your [guidance page](#).





BASIC REPORTING

-  Clear, unambiguous, professional English language used throughout.
-  Intro & background to show context. Literature well referenced & relevant.
-  Structure conforms to [PeerJ standards](#), discipline norm, or improved for clarity.
-  Figures are relevant, high quality, well labelled & described.
-  Raw data supplied (see [PeerJ policy](#)).

EXPERIMENTAL DESIGN

-  Original primary research within [Scope of the journal](#).
-  Research question well defined, relevant & meaningful. It is stated how the research fills an identified knowledge gap.
-  Rigorous investigation performed to a high technical & ethical standard.
-  Methods described with sufficient detail & information to replicate.

VALIDITY OF THE FINDINGS

-  Impact and novelty not assessed. Negative/inconclusive results accepted. *Meaningful* replication encouraged where rationale & benefit to literature is clearly stated.
-  Data is robust, statistically sound, & controlled.
-  Conclusions are well stated, linked to original research question & limited to supporting results.
-  Speculation is welcome, but should be identified as such.

Standout reviewing tips

3



The best reviewers use these techniques

Tip

Support criticisms with evidence from the text or from other sources

Example

Smith et al (J of Methodology, 2005, V3, pp 123) have shown that the analysis you use in Lines 241-250 is not the most appropriate for this situation. Please explain why you used this method.

Give specific suggestions on how to improve the manuscript

Your introduction needs more detail. I suggest that you improve the description at lines 57- 86 to provide more justification for your study (specifically, you should expand upon the knowledge gap being filled).

Comment on language and grammar issues

The English language should be improved to ensure that an international audience can clearly understand your text. Some examples where the language could be improved include lines 23, 77, 121, 128 – the current phrasing makes comprehension difficult.

Organize by importance of the issues, and number your points

1. Your most important issue
2. The next most important item
3. ...
4. The least important points

Please provide constructive criticism, and avoid personal opinions

I thank you for providing the raw data, however your supplemental files need more descriptive metadata identifiers to be useful to future readers. Although your results are compelling, the data analysis should be improved in the following ways: AA, BB, CC

Comment on strengths (as well as weaknesses) of the manuscript

I commend the authors for their extensive data set, compiled over many years of detailed fieldwork. In addition, the manuscript is clearly written in professional, unambiguous language. If there is a weakness, it is in the statistical analysis (as I have noted above) which should be improved upon before Acceptance.

A close relative of the Amazon river dolphin in marine deposits: A new Iniidae from the late Miocene of Angola

Olivier Lambert ^{Corresp., 1}, Camille Auclair ², Cirilo Cauxeiro ^{3,4}, Michel Lopez ⁴, Sylvain Adnet ²

¹ D.O. Terre et Histoire de la Vie, Institut royal des Sciences naturelles de Belgique, Brussels, Belgium

² ISEM, Université de Montpellier, Montpellier, France

³ Faculdade de Ciências, Universidade Agostinho Neto, Luanda, Angola

⁴ Geosciences, Université de Montpellier, Montpellier, France

Corresponding Author: Olivier Lambert

Email address: olivier.lambert@naturalsciences.be

Background. Thanks to their highly specialized echolocation system, a few odontocetes (toothed cetaceans) have been able to independently colonize freshwater ecosystems. Although some extant species of delphinids (true dolphins) and phocoenids (porpoises) at least occasionally migrate upstream of large river systems, they have close relatives in fully marine regions. This contrasts with the three odontocete families only containing extant species with a strictly freshwater habitat (Iniidae in South America, the recently extinct Lipotidae in China, and Platanistidae in southeast Asia). Among those, the fossil record of Iniidae includes taxa from freshwater deposits of South America, partly overlapping geographically with the extant Amazon river dolphin *Inia geoffrensis*, whereas a few marine species from the Americas were only tentatively referred to the family, leaving the transition from a marine to freshwater environment poorly understood.

Methods. Based on a partial odontocete skeleton including the cranium, discovered in late Miocene (Tortonian-Messinian) marine deposits near the estuary of the Cuanza River, Angola, we describe a new large iniid genus and species. The new taxon is compared to other extinct and extant iniids, and its phylogenetic relationships with the latter are investigated through cladistic analysis.

Results and discussion. The new genus and species *Kwanzacetes adamsi* shares a series of morphological features with *Inia geoffrensis*, including the combination of a frontal boss with nasals being lower on the anterior wall of the vertex, the laterally directed postorbital process of the frontal, the anteroposterior thickening of the nuchal crest, and robust teeth with wrinkled enamel. As confirmed with the phylogenetic analysis, this makes the new taxon the closest relative of *I. geoffrensis* found in marine deposits. The geographic origin of *K. adamsi*, on the eastern coast of South Atlantic, suggests that the transition from the marine environment to a freshwater, Amazonian habitat may have occurred on the Atlantic side of South America. This new record further increases the inioid diversity during the late Miocene, a time interval confirmed here as the heyday for this superfamily. Finally, this first description of a Neogene cetacean from inland deposits of western sub-Saharan Africa reveals the potential of this large coastal area for deciphering key steps of the evolutionary history of modern cetaceans in the South Atlantic.

**A close relative of the Amazon river dolphin in marine deposits: a new
Iniidae from the late Miocene of Angola**

**Olivier Lambert¹, Camille Auclair^{2,5}, Cirilo Cauxeiro^{3,4}, Michel Lopez⁴ and Sylvain
Adnet⁵**

¹D.O. Terre et Histoire de la Vie, Institut royal des Sciences naturelles de Belgique - Rue
Vautier 29, 1000 Brussels, Belgium;

²Rue du Docteur Jamot 11, 23250 Sardent, France;

³Universidade Agostinho Neto - Avenida 4 de Fevereiro 71, Faculdade de Ciências, Luanda,
Angola;

⁴Geosciences, Université de Montpellier – Place Eugène Bataillon, 34095 Montpellier cedex
5, France;

⁵ISEM, Université de Montpellier – Place Eugène Bataillon, 34095 Montpellier cedex 5,
France.

Corresponding author:

Olivier Lambert

olivier.lambert@naturalsciences.be

20 **ABSTRACT**

21 **Background.** Thanks to their highly specialized echolocation system, a few odontocetes
 22 (toothed cetaceans) have been able to independently colonize freshwater ecosystems.
 23 Although some extant species of delphinids (true dolphins) and phocoenids (porpoises) at
 24 least occasionally migrate upstream of large river systems, they have close relatives in fully
 25 marine regions. This contrasts with the three odontocete families only containing extant
 26 species with a strictly freshwater habitat (Iniidae in South America, the recently extinct
 27 Lipotidae in China, and Platanistidae in southeast Asia). Among those, the fossil record of
 28 Iniidae includes taxa from freshwater deposits of South America, partly overlapping
 29 geographically with the extant Amazon river dolphin *Inia geoffrensis*, whereas a few marine
 30 species from the Americas were only tentatively referred to the family, leaving the
 31 transition from a marine to freshwater environment poorly understood.

32 **Methods.** Based on a partial odontocete skeleton including the cranium, discovered in late
 33 Miocene (Tortonian-Messinian) marine deposits near the estuary of the Cuanza River,
 34 Angola, we describe a new large iniid genus and species. The new taxon is compared to
 35 other extinct and extant iniids, and its phylogenetic relationships with the latter are
 36 investigated through cladistic analysis.

37 **Results and discussion.** The new genus and species *Kwanzacetes adamsi* shares a series of
 38 morphological features with *Inia geoffrensis*, including the combination of a frontal boss
 39 with nasals being lower on the anterior wall of the vertex, the laterally directed postorbital
 40 process of the frontal, the anteroposterior thickening of the nuchal crest, and robust teeth
 41 with wrinkled enamel. As confirmed with the phylogenetic analysis, this makes the new
 42 taxon the closest relative of *I. geoffrensis* found in marine deposits. The **geographic origin** of

K. adamsi, on the eastern coast of South Atlantic, suggests that the transition from the marine environment to a freshwater, Amazonian habitat may have occurred on the Atlantic side of South America. This new record further increases the iniooid diversity during the late Miocene, a time interval confirmed here as the heyday for this superfamily. Finally, this first description of a Neogene cetacean from inland deposits of western sub-Saharan Africa reveals the potential of this large coastal area for deciphering key steps of the evolutionary history of modern cetaceans in the South Atlantic.

INTRODUCTION

Many recent works based on both morphological and molecular arguments have demonstrated and elaborated on the iterative, independent shift of echolocating toothed cetaceans (odontocetes) from marine to freshwater environments (e.g. Fordyce, 1983; Muizon, 1988; Cassens et al., 2000; Nikaido et al., 2001; Geisler et al., 2011; Geisler, Godfrey & Lambert, 2012; Bianucci et al., 2013; Gutstein, Cozzuol & Pyenson, 2014; Gutstein et al., 2014; Pyenson et al., 2015; Aguirre-Fernández et al., 2017).

The most successful extant river odontocete is the Amazon river dolphin (*Inia* spp., family Iniidae); it displays a broad distribution and genetic diversity in South American freshwater ecosystems, suggesting a long evolutionary history in this vast region (Best & da Silva, 1989; Hrbek et al., 2014). Although several species of Inioidea (superfamily including Iniidae + Pontoporiidae) from late Miocene and early Pliocene marine deposits of South and North America were tentatively referred to the Iniidae (Allen, 1941; Muizon, 1988; Cozzuol, 2010; Geisler, Godfrey & Lambert, 2012; Pyenson et al., 2015; Lambert et al.,

2017), the content of the family is still debated, either due to the fragmentary state of the type material or to the lack of clear diagnostic features. The only extinct iniid displaying the typical vertex of the cranium of the extant species is *Ischyrorhynchus vanbenedeni* Ameghino, 1891, originating from freshwater late Miocene deposits of Argentina and Brazil (Cozzuol, 2010; Gutstein, Cozzuol & Pyenson, 2014); this thus leaves unresolved the question of the marine to freshwater transition of Iniidae.

In this work we report on the description of a new iniid, based on a partial skeleton including the cranium of a relatively large dolphin from late Miocene marine deposits of Angola. Originating from a region, sub-Saharan Africa, that up to now only produced a very limited number of cetacean fossils (e.g. Andrews, 1919; Bianucci, Lambert & Post, 2007; Jacobs et al., 2016; Mourlam and Orliac, 2017; see also a detailed review in Gingerich, 2010, including a couple of records from Angola). Displaying the frontal boss typical of the extant *Inia*, the new genus and species brings elements feeding the debate on the phylogenetic relationships and palaeobiogeographic history of Iniidae.

MATERIALS AND METHODS

Nomenclatural acts: The electronic version of this article in portable document format (PDF) will represent a published work according to the International Commission on Zoological Nomenclature (ICZN), and hence the new names contained in the electronic version are effectively published under that code from the electronic edition alone. This published work and the nomenclatural acts it contains have been registered in ZooBank, the online registration system for the ICZN. The ZooBank LSIDs (life science identifiers) can

be resolved and the associated information viewed through any standard web browser by appending the LSID to the prefix <http://zoobank.org/>. The LSID for this publication is: urn:lsid: zoobank.org:pub:9488E279-A53A-4E7A-A2F7-AF8C693C208A. The online version of this work is archived and available from the following digital repositories: PeerJ, PubMed Central and CLOCKSS.

Studied specimen: The specimen consists of a partly preserved cranium (CZA 1), a detached fragment of the rostrum including both premaxillae, the right maxilla, and two teeth (CZA 2), three posterior teeth on a smaller right maxilla fragment (CZA 3), the axis (CZA 4), a more posterior cervical vertebra (CZA 5), a vertebral centrum (CZA 6), fragments of forelimb (CZA 7 and CZA 8), and fragments of ribs (CZA 9 to 16). Considering the fragmentary state of other elements, only the cranium, teeth, and cervical vertebrae are described here. Material is temporarily housed at ISEM for study, before its final return to the Universidade Agostinho Neto, Luanda, Angola.

Anatomical terminology: Terminology for cranial anatomy follows Mead & Fordyce (2009) otherwise stated.

Phylogenetic analysis: To investigate the phylogenetic relationships of the new taxon we coded CZA 1-16 in the character/taxon matrix of Post, Louwye & Lambert (2017), modified from the matrix of 324 characters by Lambert et al. (2017) (see Supplemental Information). As in the former, using PAUP 4.0a (Swofford, 2003) three outgroups (*Bos taurus*, *Hippopotamus amphibius*, and *Sus scrofa*) were defined; ordered multistate characters were scaled for a minimum length of each being one step; and a constraint tree resulting from Bayesian analysis of a molecular dataset on extant species was enforced as a backbone (see Supplemental Information). Most parsimonious trees were obtained by

heuristic search, using tree-bisection-reconnection branch swapping algorithm and ACCTRAN character-state optimization.

GEOLOGICAL SETTING

The fossil material studied here was discovered south of the estuary of the Cuanza River (Barra do Cuanza), in the Inner Kwanza basin, 74 km south of Luanda ($X = -9.359298$, $Y = 13.152918$) (Fig. 1). The Inner Kwanza basin corresponds to a salt-controlled mobile margin submitted to an overall uplift during the late Neogene that led to the continentalization of the domain and the outcropping of shelf to slope deposits along well-exposed coastal cliffs. In particular, South of Barra do Cuanza the lower to middle Miocene deposits were slightly tilted to the south during the raft tectonic and were overlapped unconformably by upper Miocene-Pliocene sands where the skeleton was discovered (Fig. 2). The lower to middle Miocene (Fig. 2: sequence 1) of the tilted block was dated by a foraminiferal and calcareous nannoplankton assemblage (Cauxeiro, 2013). It shows a partly preserved regressive sequence passing from dark to black organic-rich shales alternating with poorly graded fine to medium hummocky cross-stratified sandstone from offshore transition environment, to clayey mudstone-blue-grey marls alternations of more protected outer shelf environment on top. This series is truncated by a dark orange to brown iron-rich 50 cm-thick fossil-rich lag conglomerate reworking the previous deposits and indicating a major time gap and associate condensation episode (Fig. 2: sequence 2). This regional marine erosional surface was dated of middle Miocene (late Langhian) by Cauxeiro (2013). It is unconformably overlapped by an overall transgressive sequence

showing in the lower part 30 to 40 m thick well sorted, fine to medium beige sand, partly indurated, and intensely burrowed by Ophiomorpha (Fig. 2: sequence 3). These deposits are intersected by 2D megaripple bodies of medium to coarse sand indicating an overall northward transport by longshore currents in the upper shoreface domain. The upper part of the sequence (Fig. 2: sequence 4) is mainly composed of about 20 meters of greenish grey, intensely bioturbated clayey silt to fine sands that indicate the deepening of the depositional system towards the lower shoreface domain. The odontocete remains were discovered in the lower sand unit (Fig. 2: sequence 3), about 10 meters above the basal erosional unconformity. The skeleton elements were supposed partly connected or in situ dismembered as demonstrated by the discovery of successive vertebrae behind the skull (Fig. 3). The upper shoreface sands containing the fossil could not be dated directly, their dating thus remains relatively uncertain inside the Tortonian-Messinian interval (Cauzeiro, 2013). The top of the sedimentary pile of the cliff shows a 20 to 30 meters thick coarsening upward sequence of poorly sorted fine to coarse sand (Fig. 2 sequence 5). The base of this sequence is sharp and corresponds to a lag conglomerate of gravels and reworked bioclasts and cetacean bones. This last level probably corresponds to the fossiliferous levels evocated by Jacobs et al. (2016) 5 km north of the Cuanza River mouth, with the presence of fossil mysticete and crocodile remains. This sequence is reported to the progradation of the proto-Cuanza deltaic prism that follows the major late Miocene sea level fall during the early Pliocene highstand (Cauzeiro, Durand & Lopez, 2014).

Fossil material collected by part of the authors (ML, CC) during a fieldtrip in 2012 was excavated in the laboratory (CA) from its indurated sandy matrix with an aircsibe. It

157 consists of a partial skull with connected fragment of rostrum, some vertebrae, and
158 fragments of ribs and forelimbs.

159

160 **SYSTEMATIC PALEONTOLOGY**

161

162 Order Cetacea Brisson, 1762

163 Pelagiceti Uhen, 2008

164 Neoceti Fordyce & Muizon, 2001

165 Suborder Odontoceti Flower, 1867

166 Infraorder Delphinida Muizon, 1984

167 Superfamily Iniioidea Muizon, 1988

168 Family Iniidae Gray, 1846

169 *Kwanzacet*us, gen. nov.

170

171 **Type and only included species:** *Kwanzacet*us *adamsi*, sp. nov.

172 **Etymology:** *Kwanza* from the Kwanza basin, the area where the holotype was collected;
173 *cetus*, whale in Latin.

174 **Diagnosis:** Same as for the only included species.

175

176 *Kwanzacet*us *adamsi*, sp. nov. (Figs. 4-9, 11, 12).

177

178 **Holotype and only referred specimen:** CZA 1-16, a partial skeleton including the partly
179 preserved cranium, five teeth, the axis, a more posterior cervical vertebra, a vertebral
180 centrum, fragments of forelimb and ribs.

181 **Type locality:** Kwanza basin - South Barra do Cuanza and estuary of the Cuanza River
182 (Figs. 1-2), about 74 km south of Luanda (GPS Bc65 X= -9.359298, Y= 13.152918), Angola.

183 **Type horizon:** The holotype was discovered about 10 meters above the basal erosional
184 unconformity of an unnamed lithological unit, made of fine to medium-grained beige sand,
185 partly indurated and intensely burrowed by Ophiomorpha, which constitutes the lower
186 part of a local transgressive sequence (Fig. 2). Tortonian-Messinian interval, late Miocene
187 (see details above).

188 **Etymology:** The species name honors the English writer Douglas Adams (1952-2001), for
189 his literary work entitled *The Hitchhiker's Guide to the Galaxy*.

190 **Diagnosis of species:** This large Iniidae shares with the smaller *Brujadelphis ankylorostis*
191 Lambert, Bianucci, Urbina & Geisler, 2017 and *Isthminia panamensis* Pyenson, Vélez-Juarbe,
192 Gutstein, Little, Vigil & O'Dea, 2015 (both tentatively attributed to the family Iniidae): the
193 partial ankylosis of the premaxillae on the rostrum; with *Inia geoffrensis* (Blainville, 1817)
194 and *Ischyrorhynchus vanbenedeni*: the presence of a frontal boss, with nasals being lower
195 than the frontals on the vertex; and teeth being markedly ornamented, with wrinkled
196 enamel; with *I. geoffrensis*: the laterally directed postorbital process of the frontal; the
197 anteroposterior thickening of the nuchal crest (to an even greater extent than *I.*
198 *geoffrensis*); and the more developed left occipital protuberance (the latter being only seen
199 in part of the *I. geoffrensis* sample).

200 It further differs from *Isch. vanbenedeni* in: the lateral margin of the supraorbital
 201 process making a straight anterolaterally directed line towards the postorbital process; the
 202 nasals being anteroposteriorly longer, broadly exposed dorsally; the frontal boss being
 203 considerably lower, only a few millimeters higher than the nuchal crest; and the
 204 postglenoid process being located higher than the paroccipital process. It further differs
 205 from *I. geoffrensis* in: the lower premaxillary eminence, lacking a vertical lateral wall; the
 206 postorbital process being anteroposteriorly and transversely thick; ~~the nasals being~~
 207 ~~anteroposteriorly longer~~, broadly exposed dorsally; ~~the frontal boss being considerably~~
 208 ~~lower, only a few millimeters higher than the nuchal crest~~; the temporal crests projecting
 209 far posterior to the supraoccipital shield; and the absence of any heel on the crown of
 210 posterior maxillary teeth.

211 Among inioid species at least tentatively attributed to the family Iniidae, it further
 212 differs from *Brujadelphis ankylorostris* and *Isthminia panamensis* in: a broadly dorsally
 213 exposed squamosal fossa; and the temporal crests projecting far posterior to the
 214 supraoccipital shield; from *Meherrinia isoni* Geisler, Lambert & Godfrey, 2012 in: the
 215 presphenoid being barely exposed between the premaxillae; nasals being approximately as
 216 wide as the bony nares; the frontals on the vertex being at least as long as transversely
 217 wide; and the absence of an anterodorsomedial projection of the supraoccipital shield
 218 between the supraorbital processes; from the poorly known *Goniodelphis hudsoni* Allen,
 219 1941 in: left and right upper alveolar groove remaining distant from each other anteriorly;
 220 the absence of a markedly concave lateral margin of the premaxilla in the antorbital area;
 221 and the maxilla being roughly as wide as the premaxilla at the level of the antorbital notch
 222

DESCRIPTION AND COMPARISON

Cranium

Preservation state: The proximal part of the rostrum is only partly preserved, with most of the lateral margins incomplete; both antorbital notches are lost, as well as most of the left supraorbital region, the right preorbital region, the left lateral part of the basicranium, parts of the right squamosal, ear bones, and the most fragile bones of the ventral surface (Figs. 4-9). A part of the neural arch of a vertebra is attached in the upper part of the right temporal fossa and a smaller fragment of bone partly covers the dorsomedial region of the supraoccipital shield.

Surfaces of the bones are often considerably abraded and a thin layer of sediment is retained in a few regions, due to the low mineralization of underlying bone, making the latter extremely delicate. Low mineralization degree presumably lead to the formation of a few cavities, the largest being located on the right maxilla lateral to the vertex. As a consequence of this preservation state, part of the sutures and at least some of the cranial foramina could not be detected.

Taking account of the moderate deformation of the foramen magnum and the left temporal crest being closer to the corresponding occipital condyle than the right crest (Fig. 7), the cranium underwent some degree of differential dorsoventral crushing. Such a slight crushing may have resulted in minor changes of orientation for processes and crests.

Ontogenetic stage: Considering the closure of all cranial sutures, including the complete ankylosis of the dorsomedial suture between premaxillae on the rostrum, the complete ankylosis of the epiphyses of the post-axis cervical vertebra and limb bones (see Galatius &

Kinze, 2003), the robust aspect of cranial bones and crests, and the extensive occlusion wear facets in all preserved upper teeth (see below), the holotype CZA 1-16 is interpreted as sub-adult to adult.

General morphology: Estimated postorbital and bizygomatic widths indicate a cranial width between 280 and 290 mm (Table 1); this is in the upper part of the range for *Inia geoffrensis* (Pilleri & Gihl, 1969; pers. obs.), whose body length reaches up to 2m50 in adult males (Martin & Da Silva, 2006). The rostrum is wider than high at its preserved apex; it widens markedly towards the lost antorbital notch. The anterior part of the facial region is much wider than the posterior part, due to the abrupt narrowing of the maxilla and frontal towards the nuchal crest, leaving the temporal fossa nearly completely dorsally open (Fig. 4), as in *I. geoffrensis*. The temporal fossa is anteroposteriorly long, extending posteriorly far beyond the medial region of the supraoccipital shield due to the posterior projection of the temporal crest until the level of the occipital condyles (Fig. 5). The elevation of the facial region towards the anteroposteriorly long vertex is moderate, but abrupt, with a vertex considerably higher than in the extant pontoporiid *Pontoporia blainvillei* (Gervais & d'Orbigny, 1844) and some fossil relatives (see Muizon, 1984; Lambert & Muizon, 2013). The nuchal crest is high and greatly thickened.

Premaxilla: At the anterior end of the rostrum as preserved, which is at about 300 mm from the anterior boundary of the bony nares, the two premaxillae are dorsomedially ankylosed, with no trace of suture left; at this level the cross section of the premaxillae is semi-circular, as in *Brujadelphius ankylorostris* and *Isthminia panamensis* (Pyenson et al., 2015; Lambert et al., 2017). A clear separation of the premaxillae only occurs a short distance (32 mm) anterior to the bony nares (Fig. 4). Damaged bone in this area suggests

269 that the anterior outline of the nares was originally more U-shaped than V-shaped. At
 270 rostrum base, the dorsal surface of each premaxilla is slightly transversely convex, facing
 271 dorsolaterally. Visible on both sides, the premaxillary foramen is roughly at the same
 272 anteroposterior level as the **estimated position of the antorbital notch**, or only slightly
 273 posterior. Each foramen is followed anteriorly by a shallow anteromedial sulcus for at least
 274 35 mm. **The premaxilla** is considerably thicker, more convex lateral to the sulcus, whereas
 275 in the prenasal triangle the dorsal surface is slightly transversely convex and
 276 subhorizontal, with the medial margin barely more elevated. The posterolateral sulcus is
 277 shallow for most of its extent, reaching at least the level of the anterior margin of the bony
 278 nares (surface damaged more posteriorly), and the posteromedial sulcus is indistinct. The
 279 surface of the premaxillary sac fossa is **moderately transversely and anteroposteriorly**
 280 convex, and thickened, with a maximum height above the lateral premaxilla-maxilla suture
 281 of 9.5 mm on the left side; such a condition corresponds to a low premaxillary eminence,
 282 lower than in adults of *Inia geoffrensis* and, to a lesser extent, than in the holotype of
 283 *Brujadelphis ankylorostris*. The lateral margin of the premaxilla is straight in the rostrum
 284 base region, with a moderate divergence of right and left margins until the level of the
 285 anterior margin of the bony nares. The posterior end of each premaxilla is damaged and
 286 incomplete. On both sides sediment covers part of the maxilla along the posterolateral
 287 margin of the bony nares (Figs. 4, 9); ~~this may indicate that the premaxillae originally did~~
 288 ~~not reach the posterior margin of the nares and diverged somewhat posterolaterally, as in~~
 289 ~~some inioids~~ (e.g., *Inia geoffrensis* and *Pontoporia blainvillei*). A more complete specimen
 290 will be necessary to more precisely assess the shape and extent of the posterior end of each
 291 premaxilla. In lateral view the posterodorsal elevation of the premaxilla starts at the level

of the premaxillary foramen, but it remains weak until the preserved **end** of the premaxilla, the lateral margin of the bony nares being much lower than the top of the nasal.

The dorsolateral premaxilla-maxilla suture is closed on the rostrum, and it lacks any lateral groove, a condition differing from *Pontoporia blainvillei*.

Maxilla: At the preserved anterior end of the rostrum the maxilla is exposed lateral to the premaxilla in dorsal view (Fig. 4). At rostrum **base** the dorsal exposure of the maxilla has roughly the same width as the premaxilla, forming a wide and slightly transversely concave surface. **Only** two small dorsal infraorbital foramina opening anterolaterally could be detected **on the left side**, just behind the level of the premaxillary foramen; the anteromedial foramen has a diameter of 5 mm and the posterolateral a diameter of more than 4 mm. No other foramen is visible on the dorsal surface, but surfaces are damaged and partly covered with sediment. Posterior to the postorbital process the lateral margin of the maxilla is directed posteromedially, more than in *Brujadelphus ankylorostris* and *Isthminia panamensis*, and conspicuously elevated dorsolaterally. This elevated margin defines posterolaterally a deep fossa, limited posteriorly by the high nuchal crest and medially by the frontal and nasal on the vertex (Figs. 4, 9). This deep fossa is reminiscent of *B. ankylorostris*, *Ischyrorhynchus vanbenedeni*, *Inia geoffrensis*, and *Isth. panamensis*, but also *Hadrodelphis calvertense* Kellogg, 1966 and *Liolithax pappus* (Kellogg, 1955). The medial part of the maxilla is vertical along the vertex; on the right side the medial margin even slightly overhangs the underlying part of the bone (Fig. 9). Included in the nuchal crest the posterior margin of the left maxilla is regularly rounded, lacking any posterolateral and posteromedial angles, whereas a more conspicuous posteromedial angle is present on the right side.

On the preserved anterior part of the rostrum the ventral surface of the maxilla is roughly flat, becoming gradually more transversely convex posteriorly, until the approximate level of the antorbital notch where it is markedly convex (Figs. 6, 8). The preserved anteriormost alveoli are located just medial to the lateral margin of the maxilla; they have a transverse diameter of 10-11 mm and are separated by septa about 10 mm long. The right ventral infraorbital foramen is preserved, but the contributions of surrounding bones are not clear; it is probably margined by the frontal posterolaterally and by the lacrimojugal complex anterolaterally.

Palatine and pterygoid: Only the anteromedial part of the maxilla-palatine suture is visible, extending anterolaterally until a level 68 mm beyond the anterior limit of the pterygoid sinus fossa (Figs. 6, 8). Apices of right and left palatines are thus separated by a stripe of maxillae, at least 17 mm wide anteriorly. The ventrolateral surface of the palatine in the rostrum base is slightly transversely concave and crossed by a series of thin longitudinal grooves and crests, the latter most likely corresponding to the suture with the lost pterygoid. In this region, the pterygoid seems to be preserved only as a small scale of bone on the anteroventral corner of the anteriorly short pterygoid sinus fossa. Located posterior to the level of the antorbital notch (and about 25 mm anterior to the choanae), the anterior margin of this fossa forms a straight, laterally directed crest that turns posterolaterally 18 mm medial to the ventral infraorbital foramen. From this anterolateral corner, the pterygoid sinus fossa deepens distinctly posterodorsally, in the region just anterolateral to the choana. There, the lateral wall of the fossa is made of the partly preserved, thin lateral lamina of the palatine. Small pieces of the medial lamina of the pterygoid are preserved lateral to the choana and towards the basioccipital basin.

338 **Vomer:** The vomer is only visible ventrally: between the pterygoid sinus fossae, between
339 the choanae, and as a fragmented plate in the anterior part of the basioccipital basin (Figs.
340 6, 8).

341 **Presphenoid and cribriform plate:** Due to the narrow gap between the premaxillary sac
342 fossae, partly filled with sediment, the presphenoid is only visible at the nasal septum (Figs.
343 4, 9). The latter is acute and reaches a high level on the cribriform plate. Whereas the
344 dorsal edge of the plate is visible in dorsal view, some degree of anterodorsal projection of
345 the nasals gives the plate an anterodorsal direction, slightly overhanging the bony nares
346 and thus hiding the anterior surface of the plate in dorsal view.

347 **Nasal:** Although the sutures of the nasals with surrounding bones are difficult to follow, the
348 general shape of these bones can be described. Each nasal is markedly wider anteriorly; as
349 wide as the bony nares in their anterior region, both nasals abruptly narrow posteriorly
350 towards the posterior contact with the frontal (Figs. 4, 5, 9). Related to this strong posterior
351 narrowing, each nasal has a much longer surface of contact with the corresponding maxilla
352 than with the corresponding frontal. The convex dorsal surface of each nasal slopes
353 laterally and slightly anteriorly. The anteromedial part of this surface is somewhat abraded,
354 but a shallow and narrow internasal fossa may have been originally present. The anterior
355 margin of each nasal is only slightly anteriorly concave. The nasals of CZA 1-16 are
356 considerably reduced, anteroposteriorly shorter compared to *Atocetus* spp., *Brujadelphis*
357 *ankylorostris*, *Isthminia panamensis*, and *Liolithax pappus*, but not as short as in *Inia*
358 *geoffrensis* (Fig. 10), *Ischyrorhynchus vanbenedeni*, and to a lesser extent *Meherrinia isoni*.

359 **Frontal:** Narrow and relatively low at their contact with the nasals on the vertex, the
360 frontals widen and thicken posteriorly, reaching a maximum height at about mid-length of

their dorsal exposure and a maximum transverse width (29 mm) close to their posterior margin (Figs. 4, 5, 7, 9). Markedly higher than the nasals and nuchal crest, this prominent highest part of the frontals (frontal boss sensu Muizon, 1988) has a semi-circular outline in dorsal view, much similar to the condition in *Inia geoffrensis* (Fig. 10) and *Ischyrorhynchus vanbenedeni*; the dorsal surface is anteroposteriorly convex, with lateral margins overhanging the underlying maxilla (best seen in anterodorsal and posterodorsal views). The posterior margin of the prominence is defined by an abrupt step towards the nuchal crest; these two regions are separated by a shallow transverse groove, in a way similar to *I. geoffrensis* (with the groove being anteriorly convex in the latter).

None of the preorbital processes of the frontal is preserved, and the lateral margin of the orbit is lost on the right side. The long (35 mm) and robust right postorbital process is directed ventrally, slightly posteriorly, and distinctly laterally, with its lateral surface widely exposed in dorsal view (Figs. 4, 9), as in *I. geoffrensis*. The cross section of this process is triangular, related to the development of a high infratemporal crest along its ventromedial surface, reaching its apex (Figs. 6, 8). Just posterior to the infratemporal crest, the ventral surface of the frontal is excavated by a large and deep fossa in its medial part. Extending laterally without any defined lateral and posterolateral boundaries, this fossa is interpreted as for a large postorbital lobe of the pterygoid sinus. This lobe is comparatively large in *I. geoffrensis*, and smaller in *Pontoporia blainvillei* (Fraser & Purves, 1960). Anteromedial to the narrow, triangular medial portion of the frontal groove, another large and deep fossa is observed, presumably for an extended preorbital lobe of the pterygoid sinus. This fossa is posterolaterally margined by a high, thin plate of bone

(see orbitosphenoid below). More laterally, depressions in the ventral surface of the frontal are less clearly defined.

Lacrimojugal complex: The only preserved part of the right lacrimojugal complex is anterolateral and lateral to the ventral infraorbital foramen (Figs. 6, 8). There, an oblique lacrimal-frontal suture can be observed. A low oblique crest directed anteromedially along the preserved lateral margin of the antorbital region may correspond to the base of the styliiform part of the jugal.

Orbitosphenoid: The medialmost part of the thin plate of bone separating the frontal groove from the fossa for the preorbital lobe of the pterygoid sinus is most likely made of the orbitosphenoid (Fig. 8).

Alisphenoid: With an anteroposterior diameter of 9 mm, the foramen ovale is large (Fig. 8). It is separated from the posterior lacerate foramen by a thick bony bridge. Its anterior wall is dorsoventrally thick and anteroposteriorly narrow, followed anteriorly by a wide, only slightly concave surface, facing ventrally and slightly anterolaterally. The damaged lateral part of this surface was probably somewhat more concave, being laterally margined by an elevated subtemporal crest. The latter only extends anteriorly until a level at about mid-length of the orbital fissure.

Parietal and interparietal: The nuchal crest being anteroposteriorly thick for its whole extent (minimum thickness on right side = 25 mm; on left side = 22 mm) (Figs. 4, 5, 9), a part of it could be made of the parietals (although the frontal is markedly thickened along the nuchal crest in *Inia geoffrensis*; Fig. 10). However, all sutures are obscured in this region. Nevertheless, a small but well-defined prominence located along the sagittal axis, between the frontal boss and the posterior wall of the nuchal crest, probably corresponds

406 to part of an interparietal. A similar prominence was observed in part of the *I. geoffrensis*
 407 crania analyzed (e.g., ZMA 17771; unnumbered specimen from the MUSM collection; Fig.
 408 10).

409 **Supraoccipital:** The posterior margin of the nuchal crest overhangs the more ventral part
 410 of the supraoccipital, and the crest reaches a height of 21 mm in its medial part. Whereas
 411 on the right side this posterior margin is posteriorly concave and draws a regular curve, on
 412 the left side the anterolateral corner displays a distinctly posteriorly convex margin. A
 413 similar asymmetric occipital tuberosity was observed on the same side in several crania of
 414 *Inia geoffrensis* (e.g., unnumbered MUSM specimen; Miller, 1918, pl. 3; Van Beneden &
 415 Gervais, 1880, pl. 33; Fig. 10). As mentioned above the high temporal crests project far
 416 posteriorly, 30 mm more than the median region of the supraoccipital shield; the crests
 417 display roughly the same extent in *Ischyrorhynchus vanbenedeni* MLP 5-16 (Pilleri & Gihl,
 418 1979, pl. 6), are shorter in *Brujadelphus ankylorostis*, *I. geoffrensis*, and *Isthminia*
 419 *panamensis*, but longer in the large early delphinidans *Hadrodelphis calvertense* and
 420 *Liolithax pappus*. In posterior view right and left crests are roughly parallel for most of the
 421 height of the shield, and are relatively close to each other, reaching medially the
 422 lateralmost margin of the premaxilla and making thus the supraoccipital shield much
 423 narrower than the supraorbital region of the cranium. Between the crests the
 424 supraoccipital is dorsoventrally convex, only excavated by a shallow sagittal groove
 425 starting 40 mm above the foramen magnum and extending dorsally for more than 32 mm.
 426 Just below the nuchal crest a short, thin, but relatively high (6 mm) external occipital crest
 427 is observed, as in *I. geoffrensis*. Dorsolateral to each condyle, the dorsal condyloid fossa is
 428 shallow.

Exoccipital: The occipital condyles are separated from the neurocranium by a moderately developed condylar neck (16 mm long on the right side). Lateral to the condyle the posterior surface of the exoccipital is overhung by the prominent temporal crest (Fig. 7). Directed ventrolaterally and slightly posteriorly this surface does not reach the posterior level of the occipital condyles. Ventrally, the articulation surface for the stylohyal on the paroccipital process is a concave surface, anteroposteriorly longer than wide. Anterolateral to this feature, the anterior surface of the exoccipital is marked by a wide, ventrolaterally directed groove most likely corresponding to the paroccipital concavity (for the posterior sinus) (Fig. 8). Leading dorsomedially to a deep, bowl-shaped depression that is well separated from the posterior lacerate foramen, the groove extends also ventroposteriorly on the ventral margin of the exoccipital. The jugular notch is deeper than wide, with a minimum ventral width of 10.5 mm and a depth of 15 mm.

Basioccipital: Right and left basioccipital crests diverge markedly posterolaterally, defining a broad basioccipital basin (Figs. 6, 8); this condition may have been somewhat accentuated due to some degree of dorsoventral crushing, but it is similar to what is observed in *Inia geoffrensis* (as compared for example to the narrower basin in *Delphinus delphis* Linnaeus, 1758, not reaching laterally beyond the lateral margins of the occipital condyles). The crests are transversely thin in their anterior portion. Only preserved on the right side, a marked thickening occurs a short distance from the jugular notch; there the ventromedial surface of the crest bears a protuberance that is posteriorly defined by a transverse crest; the latter runs for a short distance (20 mm) dorsomedially, followed towards the floor of the basioccipital basin by a slight bulge of the surface. The lateral surface of the crest is excavated in a dorsomedial direction by a wide groove, leading to a

452 large elliptical fossa with a maximum diameter of 18 mm, medial to the posterior lacerate
 453 foramen. The position of this fossa relative to the posterior lacerate foramen and the
 454 foramen ovale suggests that it most likely contains the ventral carotid foramen, although it
 455 probably partly corresponds to a diverticulum of the peribullary sinus.

456 **Squamosal:** Whereas the left squamosal is not preserved, the right zygomatic process is
 457 nearly completely lost; considering the anteroposterior level of the postorbital process of
 458 the frontal and the long temporal fossa, this process was most likely elongated. The
 459 mandibular fossa is wide (more than 35 mm), nearly transversely flat, and facing
 460 anteroventrally (Figs. 6, 8). The medialmost part of the postglenoid process is a thin,
 461 transversely directed crest. The preserved section of the lateral part of the process
 462 indicates that it was considerably anteroposteriorly thicker. Medial to the mandibular fossa
 463 the large tympanosquamosal recess is triangular in outline. The recess may have extended
 464 posterolaterally, posterior to the postglenoid process, as a deep and narrow groove, as for
 465 example in *Brujadelphis ankylorostris* and *Liolithax pappus* CMM-V-3780. However, this
 466 area is poorly preserved and the external auditory meatus cannot be outlined. The
 467 falciform process of the squamosal is reduced to a low, oblique crest medial to the
 468 tympanosquamosal recess; this crest is only slightly swollen at the anteroposterior level of
 469 the foramen ovale. From this level, the squamosal extends for a short distance anteriorly as
 470 a thin plate. This plate being incomplete, a contact with a lost lateral lamina of the
 471 pterygoid (as in *Pontoporia blainvillei*) cannot be completely excluded.

472 The posttympanic process of the squamosal is characterized by a deeply concave,
 473 posterolaterally-facing surface, overhung by a thick prominence of the supramastoid crest.
 474 A similar prominence is observed in various early diverging delphinidans, including *B.*

475 *ankylorostris*, *Inia geoffrensis*, *L. pappus*, and *Macrokentriodon morani* Dawson, 1996(see
476 Lambert et al., 2017).

477 The squamosal fossa is extremely wide (Figs. 4, 9); the distance from the medial
478 surface of the temporal fossa to the lateralmost margin of the squamosal fossa is at least 64
479 mm. The floor of the fossa is transversely concave and slightly anteroposteriorly concave
480 for the anterior two thirds of its length. No deep depression is observed in the fossa,
481 different from the condition in *L. pappus* CMM-V-3780.

482

483 **Upper teeth**

484 Five upper teeth are partly preserved, including two in situ in the right maxilla at about
485 160-190 mm anterior to the level of the antorbital notch and three in a detached, more
486 posterior fragment of the right maxilla (Fig. 11). The maximum transverse diameter of the
487 robust crown ranges from 8.7 to 9.6 mm in the anterior teeth to 9.5 to 10.5 mm in the
488 posterior teeth. In one of the better preserved anterior teeth the height of the crown only
489 reaches 11.4 mm, meaning that these crowns are not significantly longer than wide. A long
490 (26 mm), posterodorsally directed root is preserved for one of the posterior teeth. The
491 enamel on the crown of all the teeth is covered with deep longitudinal crests and grooves
492 (wrinkled enamel); this ornamentation is more similar to *Inia geoffrensis* and
493 *Ischyrorhynchus vanbenedeni* (see MLP 5-18), stronger than in the few other early diverging
494 delphinidans displaying some ornamentation (e.g., *Brujadelphis ankylorostris* and *Isthminia*
495 *panamensis*). The lingual side of the crown of all the preserved teeth lacks any heel, a clear
496 difference with *I. geoffrensis*, and no accessory denticles are observed. Although the
497 preservation state is not optimal, the five teeth display a crown that is truncated along its

mesial to mesolingual side: from a relatively shallow occlusion facet in one posterior tooth to the removal of up to half the crown in several other teeth, a condition that is also observed for example in *Liolithax pappus* USNM 15985, but not in the studied specimens of *I. geoffrensis*. This pattern indicates extensive attritional (tooth to tooth) wear, at least in the posterior part of the jaws, for this individual.

Cervical vertebrae

Axis (Fig. 12A-D; Table 2): Both transverse processes are incomplete and the top of the neural arch is missing. The axis was not fused to the atlas and C3. The odontoid process is short, only slightly longer anteriorly than the anterior articular facets. A sagittal keel marks the ventral surface of the centrum. The posterior articular surface is deeply concave. The base of the transverse process is dorsoventrally high and the process was originally longer than in *Inia geoffrensis* (see Van Beneden & Gervais, 1880; Miller, 1918). The pedicle is anteroposteriorly long (minimum length 22 mm).

Other cervical vertebra (Fig. 12E-F, Table 2): This vertebra is nearly complete, only missing the distal part of the left transverse process and the lateral part of the left pre- and postzygophysis. The unfused centrum is anteroposteriorly short, with a pentagon-shaped outline in anterior view. Whereas the anterior articular surface is roughly flat, the posterior surface is slightly concave. A keel is present on the ventral surface of the centrum. With a maximum length at mid-height of the centrum, the transverse process is made of a thin blade, markedly curved anterodorsally and anteroventrally (anterior surface being dorsoventrally concave). The base of the process is pierced by a medium-size vertebral arterial canal (maximum transverse diameter of right foramen 8.5 mm). The neural

canal is roughly triangular, lower than the height of the centrum. The short pedicles are transversely wide and anteroposteriorly flattened. The better-preserved right prezygapophysis is a roughly flat surface, facing anterodorsally and slightly medially. The neural arch is slender, with only a low protuberance for the neural spine. Proportions and position of the transverse process and vertebral arterial canal are closer to C3 in *Inia geoffrensis* (see Miller, 1918), but with a smaller vertebral arterial canal medial to a more extended lateral part of the transverse process. Good similarities are also noted with C4 of *Pontoporia blainvillei* (Van Beneden & Gervais, 1880; OL, pers. obs.). This cervical is thus interpreted as a C3 or C4, pending the discovery of a more complete vertebral column of *Kwanzacetes adamsi*.

PHYLOGENETIC ANALYSIS

Similarly to the cladistic analyses by Post, Louwye & Lambert (2017), preliminary tests yielded highly volatile relationships for several Neogene inioids and other early delphinidans characterized by fragmentary type material; pending the discovery of more complete specimens, including the basicranium and ear bones, these taxa were removed from the analysis leaving a set of 101 operational taxonomic units. Our final heuristic search resulted in a single most parsimonious tree (score 1632,73 steps, consistency index 0.16, and retention index 0.57; Fig. 13; Supplemental Information).

Focusing on early diverging delphinidans (complete tree in Supplemental Information), the obtained topology differs from Post, Louwye & Lambert (2017) in *Rudicetus squalodontoides* Capellini, 1878 being sister-group to *Delphinodon dividum* True

1912 instead of *Kentriodon pernix* Kellogg, 1927, *Albireo whistleri* Barnes, 1984 being surprisingly wedged between *Tagicetus joneti* Lambert, Estevens & Smith, 2015 and the clade grouping Lipotidae and Iniioidea, *Atocetus* spp. diverging before Iniidae + Pontoporiidae, and *Scaldiporia vandokkumi* Post, Louwye & Lambert, 2017 being more closely related to *Inia* than to *Pontoporia*. Several 'kentriodontids' are thus recovered as stem delphinidans whereas others are closer to Lipotidae + Iniioidea or to Iniioidea, similarly to the trees of Lambert et al. (2017) and Post, Louwye & Lambert (2017). For our sample, Iniidae includes *Brujadelphis ankylorostris*, *Ischyrorhynchus vanbenedeni*, *Inia geoffrensis*, and *Kwanzacetus adamsi*; the attribution of *S. vandokkumi* to this family should be treated with caution, this species having been previously referred to the Pontoporiidae based on shared morphological features and phylogenetic analysis (Post, Louwye & Lambert, 2017). Among Iniidae, *K. adamsi* is sister-group to *I. geoffrensis*, whereas *Isch. vanbenedeni* is both temporally and geographically closer to the latter.

DISCUSSION

Systematics and phylogeny: *Kwanzacetus adamsi* shares morphological features with several early delphinidans and inioids: a deep fossa in the maxilla between the vertex and the elevated lateral margin of the supraorbital process (e.g., *Brujadelphis ankylorostris*, *Hadrodelfis calvertense*, *Ischyrorhynchus vanbenedeni*, *Inia geoffrensis*, *Isthminia panamensis*, and *Liolithax pappus*); an anteroposteriorly long temporal fossa (e.g., *B. ankylorostris*, *H. calvertense*, *Isch. vanbenedeni*, *I. geoffrensis*, and *L. pappus*); the temporal crest projected posteriorly beyond the supraoccipital shield (e.g., *H. calvertense*, *Isch.*

vanbenedeni, and *L. pappus*); and a broadly dorsally exposed squamosal fossa, more so than in lipotids (e.g., *H. calvertense*, *Isch. vanbenedeni*, *I. geoffrensis*, *Kampholophos serrulus* Rensberger, 1969, and *L. pappus*).

It shares additional features with part of the inioids: low premaxillary eminences (also seen in several phocoenids) and the premaxilla probably not contacting the nasal (also seen in some lipotids and many delphinoids).

Among inioids, it shares one additional character with *B. ankylorostis* and *Isth. panamensis*: partial ankylosis of the premaxillae on rostrum. It shares with *I. geoffrensis* and *Isch. vanbenedeni*: the combination of a frontal boss with nasals being lower than the frontals on the vertex (also seen phocoenids); and the proportionally robust teeth being markedly ornamented, with wrinkled enamel. Finally it shares with *I. geoffrensis*: the laterally directed postorbital process of the frontal (unknown in *Isch. vanbenedeni*); the anteroposterior thickening of the nuchal crest (even more than in the latter); the more developed left occipital protuberance (only observed in some specimens of *I. geoffrensis*) (Fig. 10).

The attribution of *Kwanzacetes adamsi* to the family Iniidae and its close relationships with *I. geoffrensis* and *Isch. vanbenedeni* are well supported by our phylogenetic analysis. Additional morphological information on the new taxon, for example on the ear bones (not preserved in the holotype) will potentially bring further support to our hypothesis.

This new inioid genus and species further increases the inioid diversity during the late Miocene, a time interval confirmed here as by far the heyday for this superfamily. Indeed, a vast majority of the extinct inioids are found in Tortonian and Messinian deposits

(e.g. Cozzuol, 2010; Gutstein, Cozzuol & Pyenson, 2014; Murakami, 2016; Post, Louwye & Lambert, 2017; Di Celma et al., 2017).

Palaeoecology and palaeobiogeography: The morphological similarities of this presumably marine species with the two known freshwater iniids (the extant *Inia geoffrensis* and the late Miocene *Ischyrorhynchus vanbenedeni*) at the level of the dentition (robustness and ornamentation of teeth), size and outline of the temporal fossa, and extent of the temporal and nuchal crests suggests at least some degree of ecological/functional anatomy overlap, for prey types, feeding strategies, and presumably locomotion. Note however the deep occlusion facets and lack of any heel on the crowns of posterior maxillary teeth in *Kwanzacetes adamsi*, two significant differences with *I. geoffrensis*. In this context of potential partial ecological overlap, the asymmetric development of the left occipital protuberance observed in both *I. geoffrensis* and *K. adamsi* may indicate a similar degree of behavioral motor asymmetry (or laterality), a phenomenon reported in many cetaceans (review in Platto et al., 2017). Interestingly, although no clear correlation has been demonstrated with laterality, four species of freshwater dolphins, including *I. geoffrensis*, have been reported performing side-swimming (Renjun et al., 1994; Platto et al., 2017). The preference for one side during swimming and/or feeding may explain the presence of a larger left occipital protuberance, for stronger neck muscles (*M. semispinalis capitis* or *rectus capitis posterior major*), **presumably** in the last common ancestor of *I. geoffrensis* and *K. adamsi*.

The record of a close relative of *I. geoffrensis* in marine deposits from the eastern coast of South Atlantic further corroborates the hypothesis that part of the early evolution

613 of the lineage of the latter (after the split with Pontoporiidae) occurred in the marine
 614 environment (Pyenson et al., 2015). Alternatively, *Kwanzacetes adamsi* may represent a
 615 less likely ecological reversal to a marine habitat, following the middle to early late
 616 Miocene colonization of freshwater habitats by iniids in South America (as proposed for an
 617 other late Miocene inioid from Panama; Pyenson et al. 2015). The oldest iniid remains from
 618 freshwater deposits of South America indeed come from late Miocene levels of Entre Rios
 619 province (Paraná Basin, Argentina) and Acre state (Brazil) localities (Cozzuol, 2010;
 620 Gutstein, Cozzuol & Pyenson, 2014). A better-constrained chronostratigraphic context for
 621 the holotype of *K. adamsi* and for South American iniid fossils would provide a more
 622 precise temporal framework.

623 Interestingly, three other late Miocene marine relatives of *I. geoffrensis* (*Brujadelphis*
 624 *ankylorostris*, *Isthminia panamensis*, and *Meherrinia isoni*) were discovered in different
 625 geographic areas (southeast Pacific, Caribbean Sea, and North Atlantic; Geisler, Godfrey &
 626 Lambert, 2012; Pyenson et al., 2015; Lambert et al., 2017; Post, Louwye & Lambert, 2017).
 627 *K. adamsi* being interpreted here as morphologically closer to *I. geoffrensis* than any of the
 628 three species mentioned above, this may indicate that the transition from a marine
 629 environment to the strictly freshwater Amazonian habitat of the latter did occur on the
 630 Atlantic side of South America. This hypothesis is further supported by the fact that some of
 631 the oldest iniid remains from South America were found in an area (Paraná Basin)
 632 relatively close to the Atlantic coast (Gutstein, Cozzuol & Pyenson, 2014) and that the Acre
 633 area, where other late Miocene iniid fossils were discovered, may have been connected
 634 with the South Atlantic by a large river system since about 10 Ma (onset of Amazon fan;
 635 Hoorn et al., 2010). It is also worth mentioning that the only surviving member of iniids'

sister-group, *Pontoporia blainvillei* (franciscana), lives along the eastern coast of South America (Brownell, 1989). We anticipate that new finds from both coasts of the South Atlantic will most likely shed further light on this still poorly understood transition. In a broader context, the first description of a Neogene cetacean from inland deposits of western sub-Saharan Africa (see review in Gingerich, 2010) reveals the potential of this large coastal area for deciphering key steps of the evolutionary history of cetaceans in the South Atlantic.

CONCLUSIONS

- Based on a partial dolphin skeleton discovered in marine deposits from the late Miocene (Tortonian - Messinian) of Angola, southwestern Africa, we describe a new genus and species, *Kwanzacetus adamsi*.

- The new taxon is referred to the family Iniidae, and among iniids it shares several cranial (e.g. frontal boss) and dental features (e.g. wrinkled enamel) with the extant Amazon river dolphin *Inia geoffrensis*.

- Confirmed by our phylogenetic analysis, the close relationship with the latter species suggests that iniids' marine to freshwater transition may have occurred during the middle to late Miocene along the Atlantic coast of South America.

- Finally, this first neocete taxon described from the Neogene of Angola reveals the potential of the southeastern Atlantic area for elucidating some crucial stages of cetacean evolutionary history.

659 **Institutional abbreviations**

660 **CMM** Calvert Marine Museum, Solomons, Maryland, USA
 661 **CZA** Universidade Agostinho Neto, Luanda, Angola (CZA in reference to the Cuanza
 662 River)
 663 **IRSNB** Institut Royal des Sciences Naturelles de Belgique, Brussels, Belgium
 664 **ISEM** Institut des Sciences de l'Evolution Montpellier, France
 665 **MLP** Museo de La Plata, La Plata, Argentina
 666 **MNHN** Muséum National d'Histoire Naturelle, Paris, France
 667 **MUSM** Museo de Historia Natural, Universidad Nacional Mayor de San Marco, Lima, Peru
 668 **NMR** Natuurhistorisch Museum Rotterdam, Rotterdam, The Netherlands
 669 **USNM** National Museum of Natural History, Smithsonian Institution, Washington, D.C., USA
 670 **ZMA** Zoölogisch Museum Amsterdam, The Netherlands

671

672 **ACKNOWLEDGEMENTS**

673

674 We wish to thank Sébastien Bruaux (IRSNB, Brussels, Belgium), Stephen J. Godfrey and
 675 John R. Nance (CMM, Solomons, USA), Christian de Muizon and Christine Lefèvre (MNHN,
 676 Paris, France), Rodolfo Salas-Gismondi, Mario Urbina and Rafael Varas-Malca (MUSM, Lima,
 677 Peru), Henry van der Es (NMR, Rotterdam, The Netherlands), David J. Bohaska, Charles W.
 678 Potter, and Nicholas
 679 D. Pyenson (USNM, Washington DC, USA) for access to collections under their care;
 680 Giovanni Bianucci (Università di Pisa, Italy) for providing photos of skull material of
 681 *Ischyrorhynchus vanbenedeni* at MLP; Giovanni Bianucci, Christian de Muizon, and Klaas

Post for fruitful discussions on various aspects of iniooid evolution; Etienne steurbaut (IRSNB, Brussels, Belgium) and Stephen Louwye (Universiteit Gent, Belgium) for testing the microfossil content of sediment samples associated to the dolphin skull; Eddy Metais, Christian Seyve, and Tatiana Tavarez (Total Exploration Production Angola, Luanda, Angola), António Olímpio and Neuza Mulanda (Agostinho Neto University, Luanda, Angola) for their help during fieldtrips and logistics; and Sébastien Enault (ISEM Montpellier - Kraniata.com, France) for constructive comments on a first draft of the paper.

ADDITIONAL INFORMATION AND DECLARATIONS

Funding

This discovery was made in March 2012, during the PhD research work of Cirilo Cauxeiro on the sedimentology and stratigraphic architecture of the Kwanza basin, funded by TOTAL Exploration Production Angola (TEPA).

New Species Registration

The following information was supplied regarding the registration of a newly described genus and species:

Publication: urn:lsid:zoobank.org:pub:9488E279-A53A-4E7A-A2F7-AF8C693C208A

Kwanzacetus: urn:lsid:zoobank.org:act:A9919C85-25B8-4D43-8C9B-9C2DC0185599

Kwanzacetus adamsi: urn:lsid: zoobank.org:act:09A29C2F-1CF1-45CA-9944-

0AFE97759D21

Supplemental Information

Supplemental information for this article can be found online at ...

REFERENCES

Aguirre-Fernández G, Mennecart B, Sánchez-Villagra MR, Sánchez R, Costeur L. 2017.

A dolphin fossil ear bone from the northern Neotropics insights into habitat transitions in iniid evolution. *Journal of Vertebrate Paleontology* **37**:E 1315817 DOI 10.1080/02724634.2017.1315817.

Allen GM. 1941. A fossil river dolphin from Florida. *Bulletin of the Museum of Comparative Zoology* **89**: 1-8.

Andrews C. 1919. A description of new species of zeuglodont and of leathery turtle from the Eocene of southern Nigeria. *Journal of Zoology* **89**:309-319.

Best RC, da Silva VMF. 1989. Amazon river dolphin, Boto. *Inia geoffrensis* (de Blainville, 1817). In Ridgway SH, Harrison R, eds. *Handbook of marine mammals, vol. 4: river dolphins and the larger toothed whales*. London, Academic Press, 1-23.

Bianucci G, Lambert O, Post K. 2007. A high diversity in fossil beaked whales (Odontoceti, Ziphiidae) recovered by trawling from the sea floor off South Africa. *Geodiversitas* **29**:5-62.

Bianucci G, Lambert O, Salas-Gismondi R, Tejada J, Pujos F, Urbina M, Antoine P-O. 2013. A Miocene relative of the Ganges river dolphin (Odontoceti, Platanistidae) from the Amazonian Basin. *Journal of Vertebrate Paleontology* **33**:741-745 DOI 10.1080/02724634.2013.734888.

- 728 **Brownell Jr RL. 1989.** Franciscana *Pontoporia blainvillei* (Gervais and d'Orbigny, 1844).
729 In: Ridgway SH, Harrison R, eds. *Handbook of marine mammals, vol. 4: river dolphins and*
730 *the larger toothed whales*. London: Academic Press, 45-67.
- 731 **Cassens I, Vicario S, Waddell VG, Balchowsky H, Van Belle D, Ding W, Chen F, Mohan**
732 **RSL, Simoes-Lopes PC, Bastida R, Meyer A, Stanhope MJ, Milinkovitch MC. 2000.**
733 Independent adaptation to riverine habitats allowed survival of ancient cetacean
734 lineages. *Proceedings of the National Academy of Sciences* **97**:11343-11347 DOI
735 10.1073/pnas.97.21.11343
- 736 **Cauxeiro C. 2013.** Architecture stratigraphique du prisme néogène de La Cuanza, Angola
737 et relations avec les mouvements verticaux, 307 p. *Unpublished Ph.D. Thesis*, University
738 of Montpellier, France.
- 739 **Cauxeiro C, Durand J, Lopez M. 2014.** Stratigraphic architecture and forcing processes of
740 the late Neogene Miradouro da Lua sedimentary prism, Cuanza Basin, Angola. *Journal of*
741 *African Earth Sciences* **95**:77-92 DOI 10.1016/j.jafrearsci.2014.01.013.
- 742 **Cozzuol, M. 2010.** Fossil record and evolutionary history of Iniioidea. In Ruiz-Garcia M,
743 Shostell J, eds. *Biology, evolution and conservation of river dolphins within South America*
744 *and Asia*. New York: Nova Science Publishers, 193-217.
- 745 **Di Celma C, Malinverno E, Bosio G, Collareta A, Gariboldi K, Gioncada A, Molli G, Basso**
746 **D, Varas-Malca RM, Pierantoni PP, Villa IM, Lambert O, Landini W, Sarti G,**
747 **Cantalamessa G, Urbina M, Bianucci G. 2017.** Sequence stratigraphy and paleontology
748 of the upper Miocene Pisco Formation along the western side of the lower Ica Valley (Ica
749 desert, Peru). *Rivista Italiana di Paleontologia e Stratigrafia* **123**:255-273 DOI
750 10.13130/2039-4942/8373.

- 751 **Fordyce RE. 1983.** Rhabdosteid dolphins (Mammalia: Cetacea) from the Middle Miocene,
752 Lake Frome area, South Australia. *Alcheringa* 7:27-40.
- 753 **Fraser FC, Purves PE. 1960.** Hearing in cetaceans: Evolution of the accessory air sacs and
754 the structure of the outer and middle ear in recent cetaceans. *Bulletin of the British*
755 *Museum (Natural History), Zoology* 7:1-140.
- 756 **Galatius A, Kinze CC. 2003.** Ankylosis patterns in the postcranial skeleton and hyoid
757 bones of the harbour porpoise (*Phocoena phocoena*) in the Baltic and North Sea.
758 *Canadian Journal of Zoology* 81:1851-1861 DOI 10.1139/z03-181.
- 759 **Geisler JH, McGowen MR, Yang G, Gatesy J. 2011.** A supermatrix analysis of genomic,
760 morphological, and paleontological data for crown Cetacea. *BMC Evolutionary Biology*
761 11:1-22 DOI 10.1186/1471-2148-11-112.
- 762 **Geisler JH, Godfrey SJ, Lambert O. 2012.** A new genus and species of late Miocene inioid
763 (Cetacea: Odontoceti) from the Meherrin River, North Carolina, U.S.A. *Journal of*
764 *Vertebrate Paleontology* 32:198-211 DOI 10.1080/02724634.2012.629016.
- 765 **Gingerich PD. 2010.** Cetacea. In Werdelin L, Sanders WJ, eds. *Cenozoic mammals of Africa*.
766 Berkeley: University of California Press, 873–99.
- 767 **Gutstein CS, Cozzuol MA, Pyenson ND. 2014.** The antiquity of riverine adaptations in
768 Iniidae (Cetacea, Odontoceti) documented by a humerus from the Late Miocene of the
769 Ituzaingó Formation, Argentina. *The Anatomical Record* 297:1096-1102 DOI
770 10.1002/ar.22901.
- 771 **Gutstein CS, Figueroa-Bravo CP, Pyenson ND, Yury-Yañez RE, Cozzuol MA, Canals M.**
772 **2014.** High frequency echolocation, ear morphology, and the marine–freshwater

773 transition: A comparative study of extant and extinct toothed whales. *Palaeogeography,*
774 *Palaeoclimatology, Palaeoecology* **400**:62-74 DOI 10.1016/j.palaeo.2014.01.026.

775 **Hoorn C, Wesselingh FP, Ter Steege H, Bermudez MA, Mora A, Sevink J, Sanmartín I,**
776 **Sanchez-Meseguer A, Anderson CL, Figueiredo JP. 2010.** Amazonia through time:
777 Andean uplift, climate change, landscape evolution, and biodiversity. *Science* 330:927-
778 931 DOI 10.1126/science.1194585.

779 **Hrbek T, da Silva VMF, Dutra N, Gravena W, Martin AR, Farias IP. 2014.** A new species
780 of river dolphin from Brazil or: how little do we know our biodiversity. *PLoS ONE*
781 **9**:e83623 DOI 10.1371/journal.pone.0083623.

782 **Jacobs LL, Polcyn MJ, Mateus O, Schulp AS, Gonçalves AO, Morais ML. 2016.** Post-
783 Gondwana Africa and the vertebrate history of the Angolan Atlantic Coast. *Memoirs of*
784 *Museum Victoria* **74**:343-362.

785 **Lambert O, Muizon C de. 2013.** A new long-snouted species of the Miocene pontoporiid
786 dolphin *Brachydelphis* and a review of the Mio-Pliocene marine mammal levels in the
787 Sacaco Basin, Peru. *Journal of Vertebrate Paleontology* **33**:709-721 DOI
788 10.1080/02724634.2013.743405.

789 **Lambert O, Bianucci G, Urbina M, Geisler JH. 2017.** A new inioid (Cetacea, Odontoceti,
790 Delphinida) from the Miocene of Peru and the origin of modern dolphin and porpoise
791 families. *Zoological Journal of the Linnean Society* **179**:919-946 DOI 10.1111/zoj.12479.

792 **Martin AR, da Silva VMF. 2006.** Sexual dimorphism and body scarring in the boto
793 (Amazon river dolphin) *Inia geoffrensis*. *Marine Mammal Science* **22**:25-33 DOI
794 10.1111/j.1748-7692.2006.00003.x

795 **Mead JG, Fordyce RE. 2009.** The therian skull: a lexicon with emphasis on the
 796 odontocetes. *Smithsonian Contributions to Zoology* **627**:1-248.

797 **Miller GS Jr. 1918.** A new river-dolphin from China. *Smithsonian Miscellaneous Collections*
 798 **68**:1-12.

799 **Mourlam MJ, Orliac MJ. 2017.** Protocetid (Cetacea, Artiodactyla) bullae and petrosals
 800 from the Middle Eocene locality of Kpogamé, Togo: new insights into the early history of
 801 cetacean hearing. *Journal of Systematic Palaeontology*:1-24. DOI:
 802 10.1080/14772019.2017.1328378.

803 **Muizon C de. 1984.** Les vertébrés de la Formation Pisco (Pérou). Deuxième partie: Les
 804 Odontocètes (Cetacea, Mammalia) du Pliocène inférieur de Sud-Sacaco. *Travaux de*
 805 *l'Institut Français d'Etudes Andines* **27**:1-188.

806 **Muizon C de. 1988.** Les relations phylogénétiques des Delphinida. *Annales de*
 807 *Paléontologie* **74**:159-227.

808 **Murakami M. 2016.** A new extinct inioid (Cetacea, Odontoceti) from the Upper Miocene
 809 Senhata Formation, Chiba, central Japan: the first record of Iniioidea from the North
 810 Pacific Ocean. *Paleontological Research* **20**:207-225 DOI 10.2517/2015PR031.

811 **Nikaido M, Matsuno F, Hamilton H, Brownel RLJ, Cao Y, Ding W, Zuoyan Z, Shedlock**
 812 **AM, Fordyce RE, Hasegawa M, Okada N. 2001.** Retroposon analysis of major cetacean
 813 lineages: The monophyly of toothed whales and the paraphyly of river dolphins.
 814 *Proceedings of the National Academy of Natural Sciences* **98**:7384-7389 DOI
 815 10.1073/pnas.121139198

- Filleri G, Gihir M. 1979.** Skull, sonar field and swimming behavior of *Ischyrorhynchus*
vanbenedeni (Ameghino 1891) and taxonomical position of the genera *Ischyrorhynchus*,
Saurodelphis, *Anisodelphis* and *Pontoplanodes*. *Investigations on Cetacea* **10**:17-70.
- Platto S, Zhang C, Pine MK, Feng W, Yang L, Irwin A, Wang D. 2017.** Behavioral laterality
in Yangtze finless porpoises (*Neophocaena asiaeorientalis asiaeorientalis*). *Behavioural*
Processes **140**:104-114 DOI 10.1016/j.beproc.2017.04.015.
- Post K, Louwye S, Lambert O. 2017.** *Scaldiporia vandokkumi*, a new pontoporiid
(Mammalia, Cetacea, Odontoceti) from the Late Miocene to earliest Pliocene of the
Westerschelde estuary (The Netherlands). *PeerJ* **5**:e3991 DOI 10.7717/peerj.3991.
- Pyenson ND, Vélez-Juarbe J, Gutstein CS, Little H, Vigil D, O'Dea A. 2015.** *Isthminia*
panamensis, a new fossil inioid (Mammalia, Cetacea) from the Chagres Formation of
Panama and the evolution of 'river dolphins' in the Americas. *PeerJ* **3**:e1227 DOI
10.7717/peerj.1227.
- Renjun L, Gewalt W, Neurohr B, Winkler A. 1994.** Comparative studies on the behaviour
of *Inia geoffrensis* and *Lipotes vexillifer* in artificial environments. *Aquatic Mammals*
20:39-39.
- Swofford DL. 2003.** PAUP*. Phylogenetic analysis using parsimony (*and other methods).
Version 4. Sinauer Associates, Sunderland, Massachusetts.
- Van Beneden P-J, Gervais P. 1880.** Ostéographie des cétacés vivants et fossiles. Paris:
Arthus Bertrand, 634 pp.

839 **FIGURE CAPTIONS**

840

841 **Figure 1. Locality of the holotype of *Kwanzacetes adamsi*.** Location map and geological
842 overview of the discovery zone of *K. adamsi* in the Kwanza basin, Angola, modified from
843 Cauxeiro, Durand & Lopez (2014).

844

845 **Figure 2. Stratigraphical context for the holotype of *Kwanzacetes adamsi*.**

846 Stratigraphical architecture of the cliff south of Barra do Cuanza where the holotype of *K.*
847 *adamsi* was discovered. A, panoramic view; B, interpreted line drawing; and C, sedimentary
848 column showing the main facies assemblage. In the lower part of the cliff, alternating
849 hummocky cross stratified sandstones, mudstones, and black shales from the lower to
850 middle Miocene (sequence 1) are slightly tilted southwards and obliquely truncated by the
851 major erosional unconformity (sequence 2). This erosional surface is overlapped by an
852 overall fining upward sequence dated from the late Miocene. This sequence shows upper
853 shoreface sand burrowed by Ophiomorpha (sequence 3) passing upwards to burrowed fine
854 sand to clayey silt from lower shoreface environment (sequence 4). The upper part of the
855 cliff is composed of an upward coarsening sequence, from fine to coarse sand and gravel
856 (sequence 5), which marks the overall progradation of the paleo-Cuanza delta during the
857 Pliocene. This sequence is floored by a marine ravinement lag deposit.

858

859 **Figure 3. Location of the holotype of *Kwanzacetes adamsi* on the cliff.** Photographs
860 before (A) and after (B) the extraction of the skull. Orange Fe-hydroxide halos in the sand
861 indicate Ophiomorpha burrowing.

862

863 **Figure 4. Dorsal view of the cranium of *Kwanzacetus adamsi*.** Photograph (A) and
864 corresponding line drawing (B) of the cranium of the holotype of *K. adamsi* CZA 1-2 in
865 dorsal view. Light grey for sediment and plaster; dark grey for attached bone fragments;
866 hatched areas for major break surfaces; dotted lines for interpretation of unclear sutures.
867 Scale bar equals 100 mm.

868

869 **Figure 5. Lateral view of the cranium of *Kwanzacetus adamsi*.** Photograph (A) and
870 corresponding line drawing (B) of the cranium of the holotype of *K. adamsi* CZA 1-2 in
871 right lateral view. Light grey for sediment and plaster; dark grey for attached bone
872 fragments; hatched areas for major break surfaces; dotted lines for interpretation of
873 unclear sutures. Scale bar equals 100 mm.

874

875 **Figure 6. Ventral view of the cranium of *Kwanzacetus adamsi*.** Photograph (A) and
876 corresponding line drawing (B) of the cranium of the holotype of *K. adamsi* CZA 1 in
877 ventral view. Light grey for sediment and plaster; hatched areas for major break surfaces.
878 Scale bar equals 100 mm.

879

880 **Figure 7. Posterior view of the cranium of *Kwanzacetus adamsi*.** Photograph (A) and
881 corresponding line drawing (B) of the cranium of the holotype of *K. adamsi* CZA 1 in
882 ventral view. Light grey for sediment and plaster; dark grey for attached bone fragments;
883 hatched areas for major break surfaces. Scale bar equals 100 mm.

884

Figure 8. Detail of the basicranium, orbit, and palate of the cranium of *Kwanzacetus*

***adamsi*.** Photograph (A) and corresponding line drawing (B) of the right side of the basicranium, orbit, and palate of the holotype of *K. adamsi* CZA 1-2 in ventrolateral and slightly anterior view. Light grey for sediment and plaster; dark grey for attached bone fragments; hatched areas for major break surfaces. Scale bar equals 100 mm.

Figure 9. Additional views of the cranium of *Kwanzacetus adamsi*. A, right

posterolateral and slightly dorsal view of the holotype of *K. adamsi* CZA 1-2; B, anterior and slightly dorsal view; C, right anterolateral and slightly dorsal view. Dotted lines for main sutures and other bone outlines. Scale bar equals 100 mm.

Figure 10. Dorsal view of the cranium of the extant iniid *Inia geoffrensis* (Amazon

river dolphin). Photograph of the facial region of the cranium of *I. geoffrensis* (unnumbered specimen MUSM) in dorsal view, showing several morphological features shared with *Kwanzacetus adamsi* and, for part of them, with other inioids and some early delphinidans (see text for details).

Figure 11. Maxillary teeth of *Kwanzacetus adamsi*. A, two more anterior right maxillary

teeth of the holotype of *K. adamsi* CZA 2 in lingual view; B, detail of one of these teeth in labiodistal view; C, three more posterior right maxillary teeth CZA 3 in lingual view; D, detail of one tooth in labiomesial view; E, detail of the same tooth in labiodistal and slightly occlusal view; F, detail of another tooth in labiomesial view. Dotted lines for deep occlusion facets. Scale bars equal 10 mm.

908

909 **Figure 12. Cervical vertebrae of *Kwanzacetes adamsi*.** A-D, axis of the holotype of *K.*
910 *adamsi* CZA 4 in anterior (A), left lateral (B), posterior (C), and ventral (D) views; E-F,
911 cervical ?C3-C4 CZA 5 in anterior (E) and right lateral (F) views. Scale bar equals 50 mm.

912

913 **Figure 13. Phylogenetic relationships of *Kwanzacetes adamsi*.** Phylogenetic tree
914 showing the relationships of *K. adamsi* with other early diverging delphinidans, as obtained
915 from our parsimony analysis of morphological data, constrained with a molecular tree as
916 backbone. Other odontocete clades are collapsed to facilitate reading. *K. adamsi* falls as an
917 iniid, displaying close relationships with the extant *Inia geoffrensis*. Stars identify species
918 with a strictly freshwater distribution (or, in the case of *Platanista gangetica*, the
919 superfamily Platanistoidea to whom it belongs).

920

921 TABLE CAPTIONS

922

923 **Table 1. Measurements (in mm) of the cranium of the iniid *Kwanzacetes adamsi* CZA**
924 **1-2 (holotype), late Miocene of Angola.** e, estimate; +, incomplete.

925

926 **Table 2. Measurements (in mm) of the cervical vertebrae of the iniid *Kwanzacetes***
927 ***adamsi* CZA 4-5 (holotype), late Miocene of Angola.** e, estimate.

Table 1(on next page)

Measurements (in mm) of the cranium of the iniid *Kwanzacetus adamsi* CZA 1-2 (holotype), late Miocene of Angola.

e, estimate; +, incomplete.

1
2

| | CZA 1-16 |
|---|----------|
| Width of rostrum at base | +130 |
| Height of rostrum at base | +65 |
| Width of premaxillae at anterior margin of right premaxillary foramen | 67 |
| Width of bony nares | e49 |
| Width of premaxillary sac fossae | e89 |
| Width of right premaxillary sac fossa | e35 |
| Width of left premaxillary sac fossa | 36 |
| Postorbital width | e281 |
| Bizygomatic width | e286 |
| Maximum anteroposterior length of right temporal fossa | 155 |
| Height of right temporal fossa from floor of squamosal fossa to top of temporal crest | 103 |
| Minimum posterior distance between maxillae across vertex | 25 |
| Distance between temporal fossae at level of medial part of nuchal crest | 121 |
| Minimum posterior distance between temporal crests | e91.5 |
| Width of occipital condyles | e96 |
| Height of right occipital condyle | 54 |
| Width of foramen magnum | e44 |

3

Table 2 (on next page)

Measurements (in mm) of the cervical vertebrae of the iniid *Kwanzacetes adamsi* CZA 4-5 (holotype), late Miocene of Angola.

e, estimate.

1
2

| | |
|---|------|
| Axis | |
| Maximum width as preserved | 127 |
| Maximum width across anterior articular facets | e106 |
| Height of left anterior articular facet | e47 |
| Width of left anterior articular facet | e37 |
| Height of posterior epiphysis | e37 |
| Width of posterior epiphysis | e63 |
| Width of neural canal | 33 |
| Maximum anteroposterior length along sagittal plane | 39 |
| Other cervical vertebra (C3 or C4) | |
| Maximum width | e106 |
| Height of anterior epiphysis | 42 |
| Width of anterior epiphysis | e49 |
| Height of posterior epiphysis | 43 |
| Width of neural canal | 37 |
| Height of neural canal | 30 |
| Anteroposterior length of centrum | 13.5 |

3

Figure 1

Locality of the holotype of *Kwanzacetus adamsi*.

Location map and geological overview of the discovery zone of *K. adamsi* in the Kwanza basin, Angola, modified from Cauxeiro, Durand & Lopez (2014).

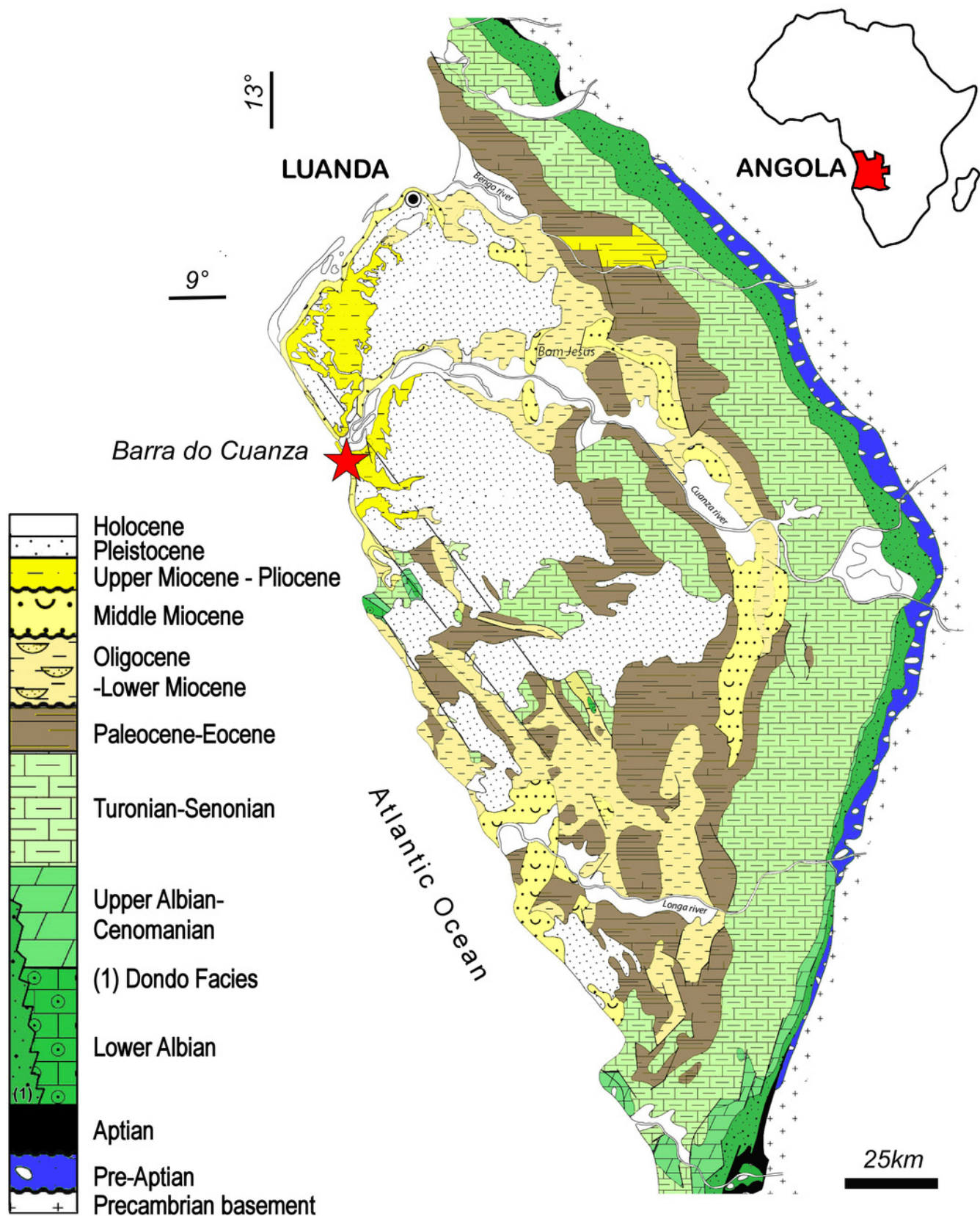


Figure 2

Stratigraphical context for the holotype of *Kwanzacetes adamsi*.

Stratigraphical architecture of the cliff south of Barra do Cuanza where the holotype of *K. adamsi* was discovered. A, panoramic view; B, interpreted line drawing; and C, sedimentary column showing the main facies assemblage. In the lower part of the cliff, alternating hummocky cross stratified sandstones, mudstones, and black shales from the lower to middle Miocene (sequence 1) are slightly tilted southwards and obliquely truncated by the major erosional unconformity (sequence 2). This erosional surface is overlapped by an overall fining upward sequence dated from the late Miocene. This sequence shows upper shoreface sand burrowed by Ophiomorpha (sequence 3) passing upwards to burrowed fine sand to clayey silt from lower shoreface environment (sequence 4). The upper part of the cliff is composed of an upward coarsening sequence, from fine to coarse sand and gravel (sequence 5), which marks the overall progradation of the paleo-Cuanza delta during the Pliocene. This sequence is floored by a marine ravinement lag deposit.

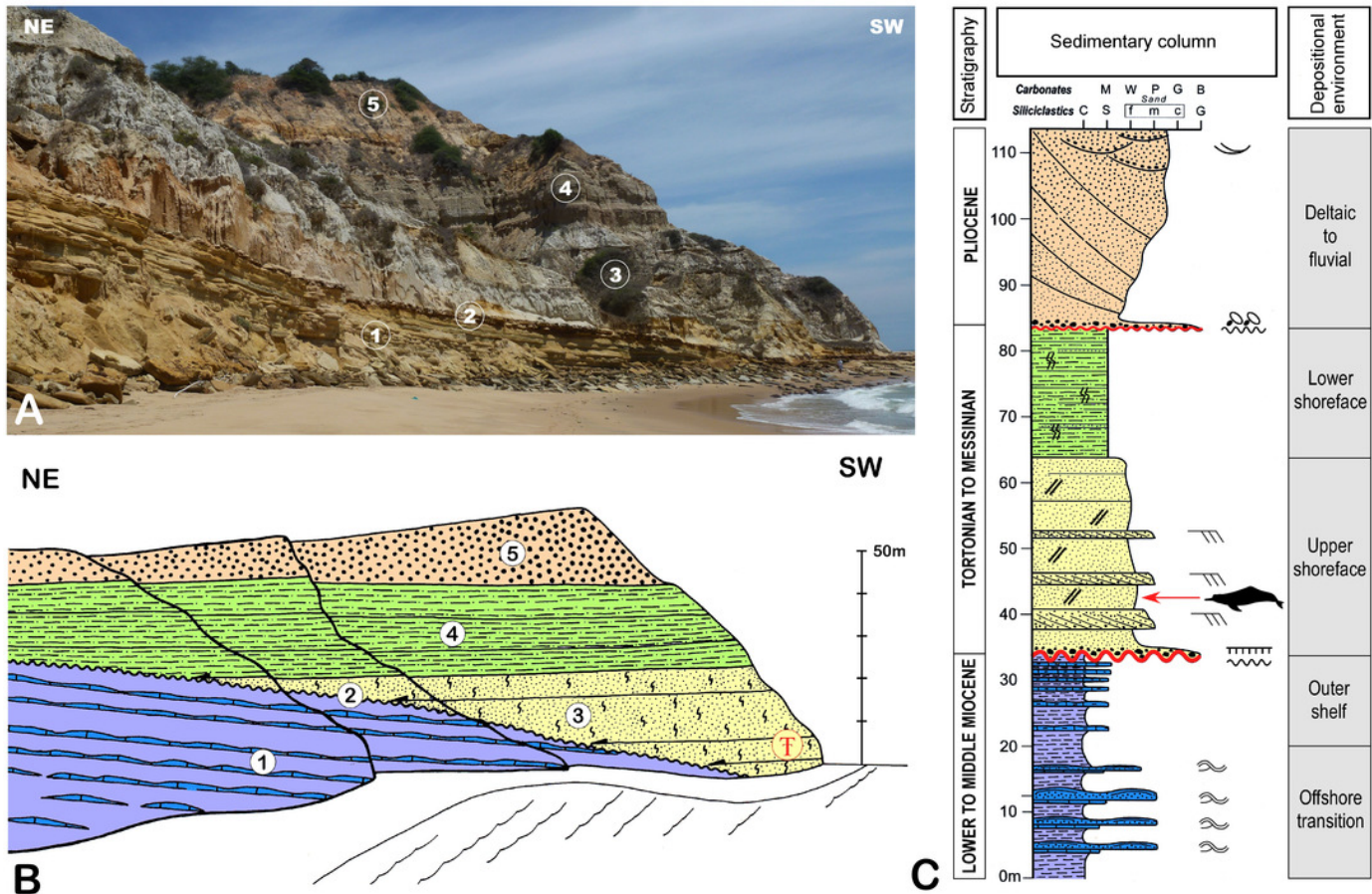


Figure 3

Location of the holotype of *Kwanzacetes adamsi* on the cliff.

Photographs before (A) and after (B) the extraction of the skull. Orange Fe-hydroxide halos in the sand indicate Ophiomorpha burrowing.



Figure 4

Dorsal view of the cranium of *Kwanzacetes adamsi*.

Photograph (A) and corresponding line drawing (B) of the cranium of the holotype of *K. adamsi* CZA 1-2 in dorsal view. Light grey for sediment and plaster; dark grey for attached bone fragments; hatched areas for major break surfaces; dotted lines for interpretation of unclear sutures. Scale bar equals 100 mm.

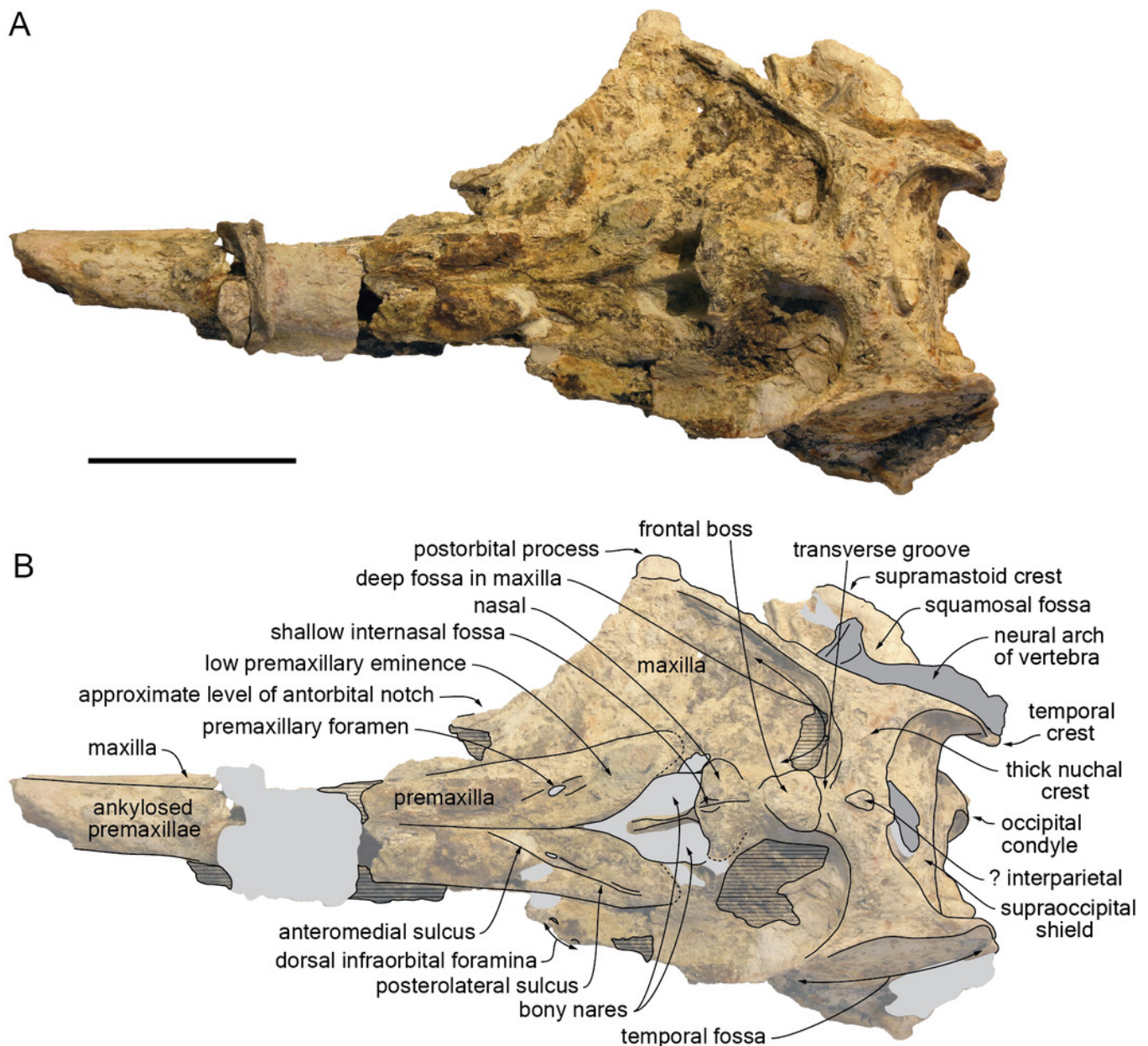


Figure 5

Lateral view of the cranium of *Kwanzacetes adamsi*.

Photograph (A) and corresponding line drawing (B) of the cranium of the holotype of *K. adamsi* CZA 1-2 in right lateral view. Light grey for sediment and plaster; dark grey for attached bone fragments; hatched areas for major break surfaces; dotted lines for interpretation of unclear sutures. Scale bar equals 100 mm.

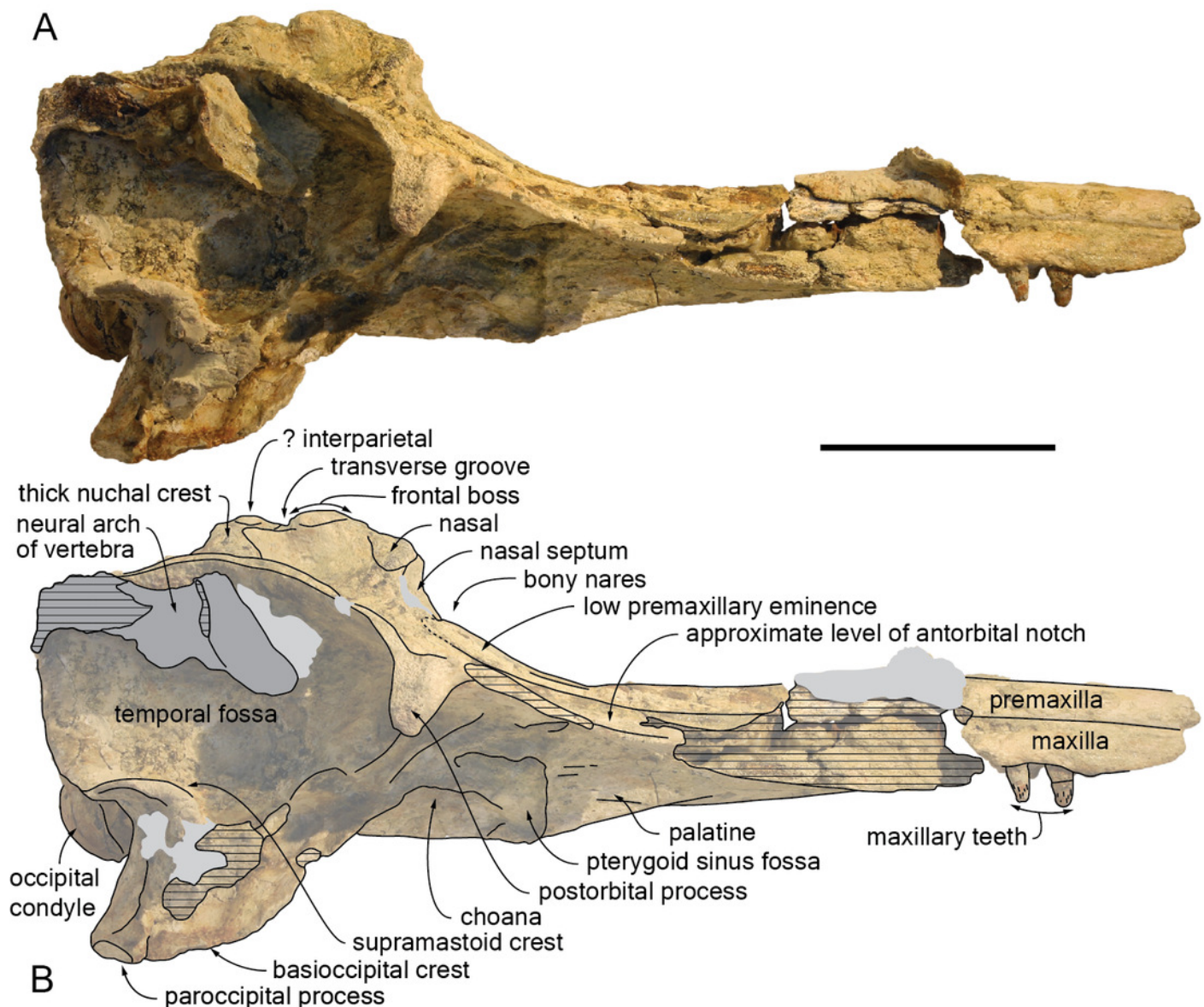


Figure 6

Ventral view of the cranium of *Kwanzacetus adamsi*.

Photograph (A) and corresponding line drawing (B) of the cranium of the holotype of *K. adamsi* CZA 1 in ventral view. Light grey for sediment and plaster; hatched areas for major break surfaces. Scale bar equals 100 mm.

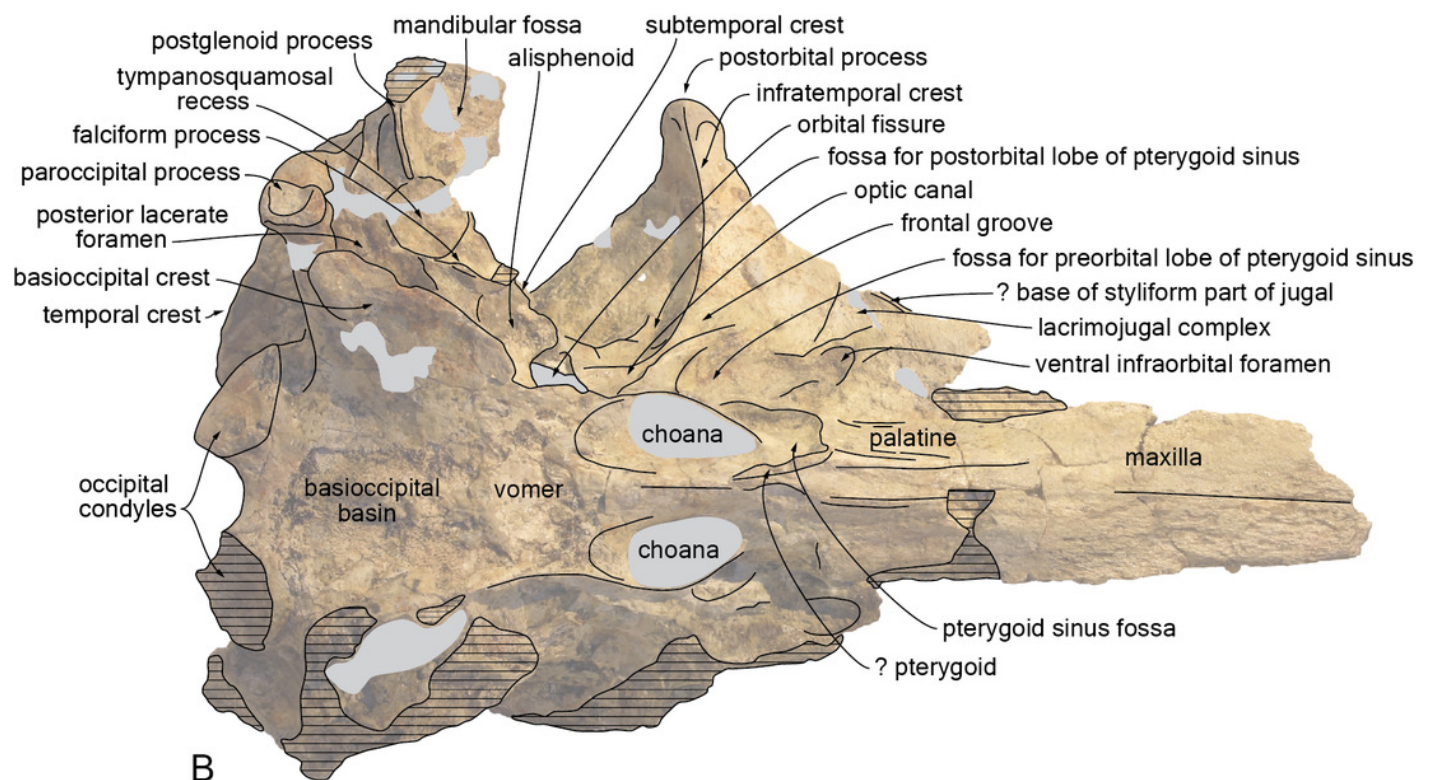
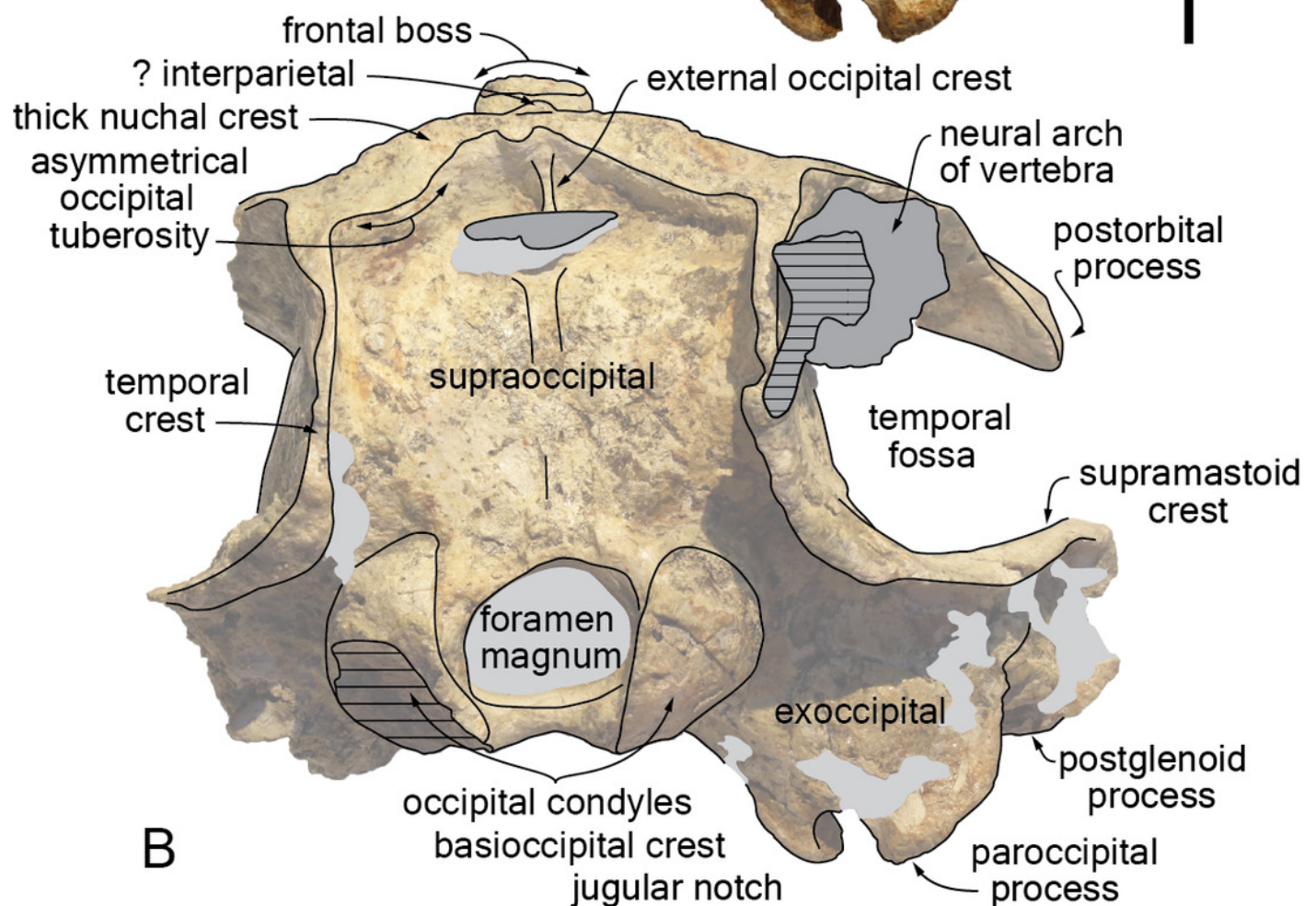


Figure 7

Posterior view of the ranium of *Kwanzacetus adamsi*.

Photograph (A) and corresponding line drawing (B) of the cranium of the holotype of *K. adamsi* CZA 1 in ventral view. Light grey for sediment and plaster; dark grey for attached bone fragments; hatched areas for major break surfaces. Scale bar equals 100 mm.

A



B

Figure 8

Detail of the basicranium, orbit, and palate of the cranium of *Kwanzacetus adamsi*.

Photograph (A) and corresponding line drawing (B) of the right side of the basicranium, orbit, and palate of the holotype of *K. adamsi* CZA 1-2 in ventrolateral and slightly anterior view. Light grey for sediment and plaster; dark grey for attached bone fragments; hatched areas for major break surfaces. Scale bar equals 100 mm.

A



B

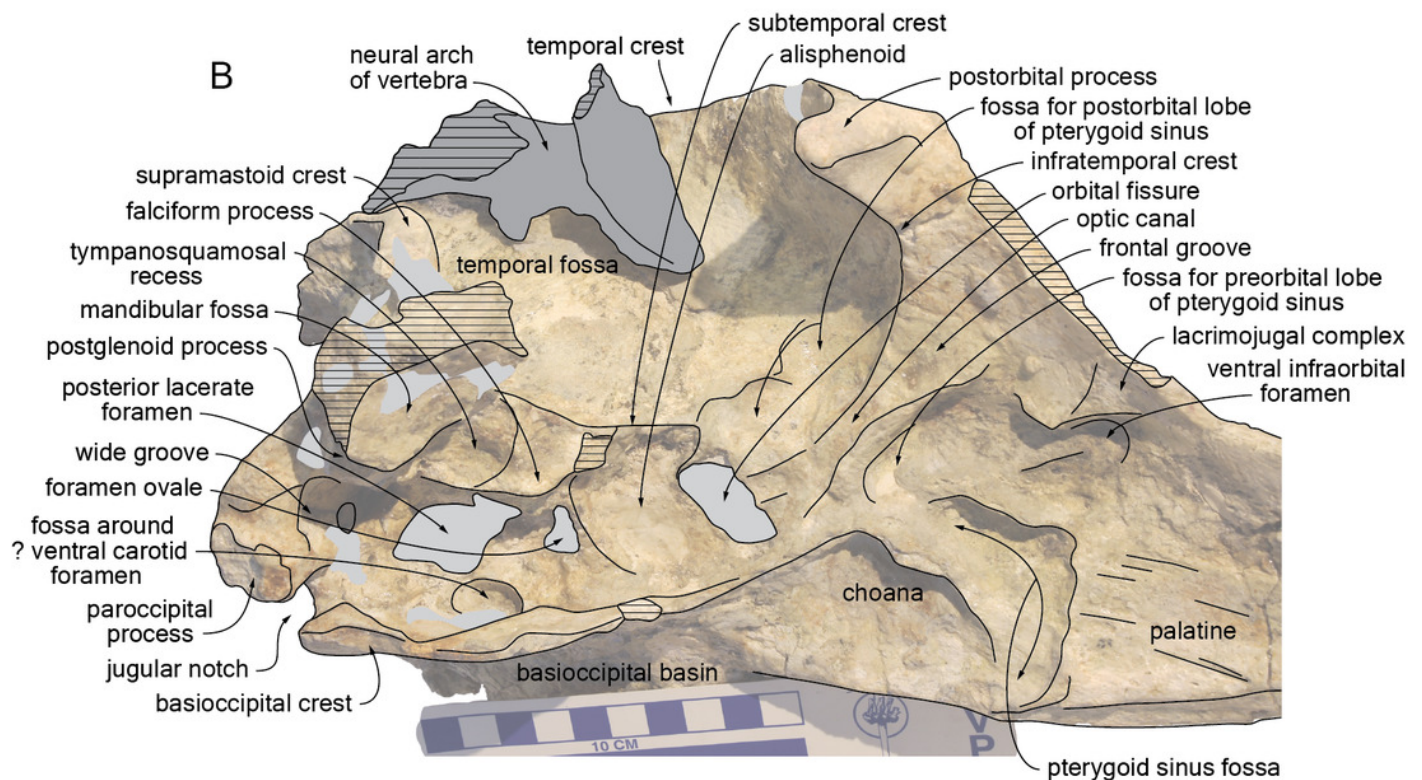


Figure 9

Additional views of the cranium of *Kwanzacetes adamsi*.

A, right posterolateral and slightly dorsal view of the holotype of *K. adamsi* CZA 1-2; B, anterior and slightly dorsal view; C, right anterolateral and slightly dorsal view. Dotted lines for main sutures and other bone outlines. Scale bar equals 100 mm.

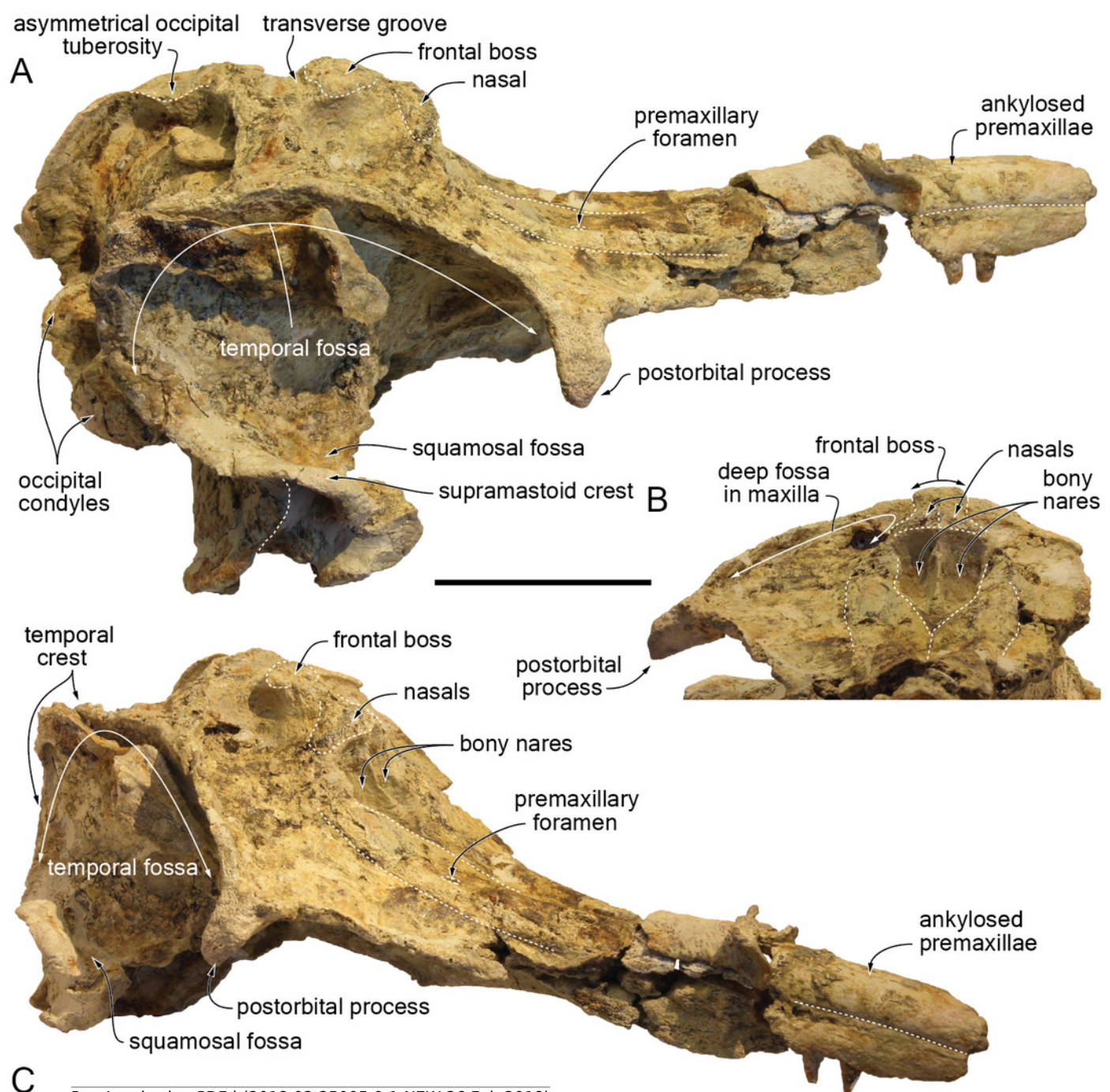


Figure 10

Dorsal view of the cranium of the extant iniid *Inia geoffrensis* (Amazon river dolphin).

Photograph of the facial region of the cranium of *I. geoffrensis* (unnumbered specimen MUSM) in dorsal view, showing several morphological features shared with *Kwanzacetus adamsi* and, for part of them, with other inioids and some early delphinidans (see text for details).

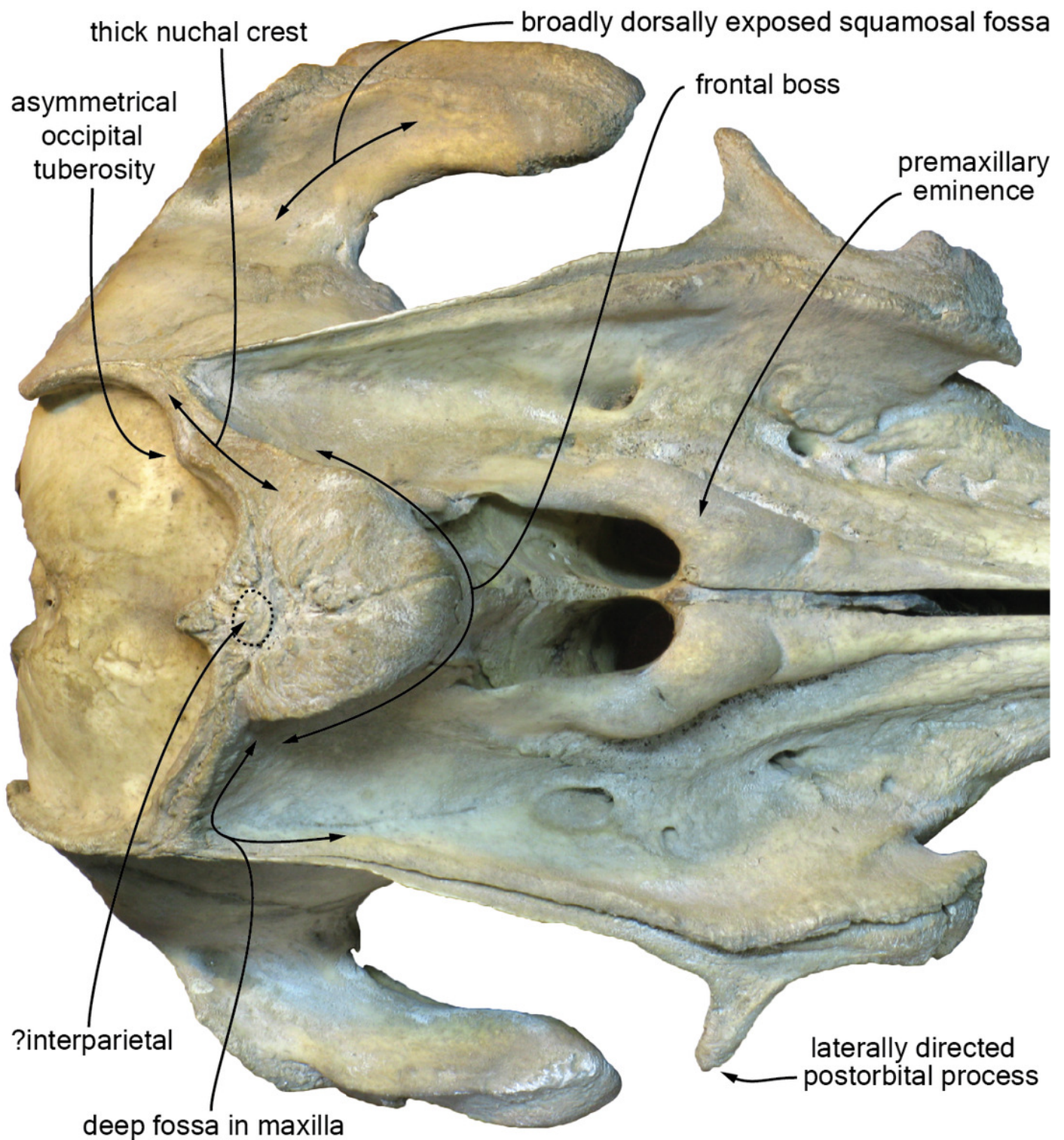


Figure 11

Maxillary teeth of *Kwanzacetus adamsi*.

A, two more anterior right maxillary teeth of the holotype of *K. adamsi* CZA 2 in lingual view; B, detail of one of these teeth in labiodistal view; C, three more posterior right maxillary teeth CZA 3 in lingual view; D, detail of one tooth in labiomesial view; E, detail of the same tooth in labiodistal and slightly occlusal view; F, detail of another tooth in labiomesial view. Dotted lines for deep occlusion facets. Scale bars equal 10 mm.

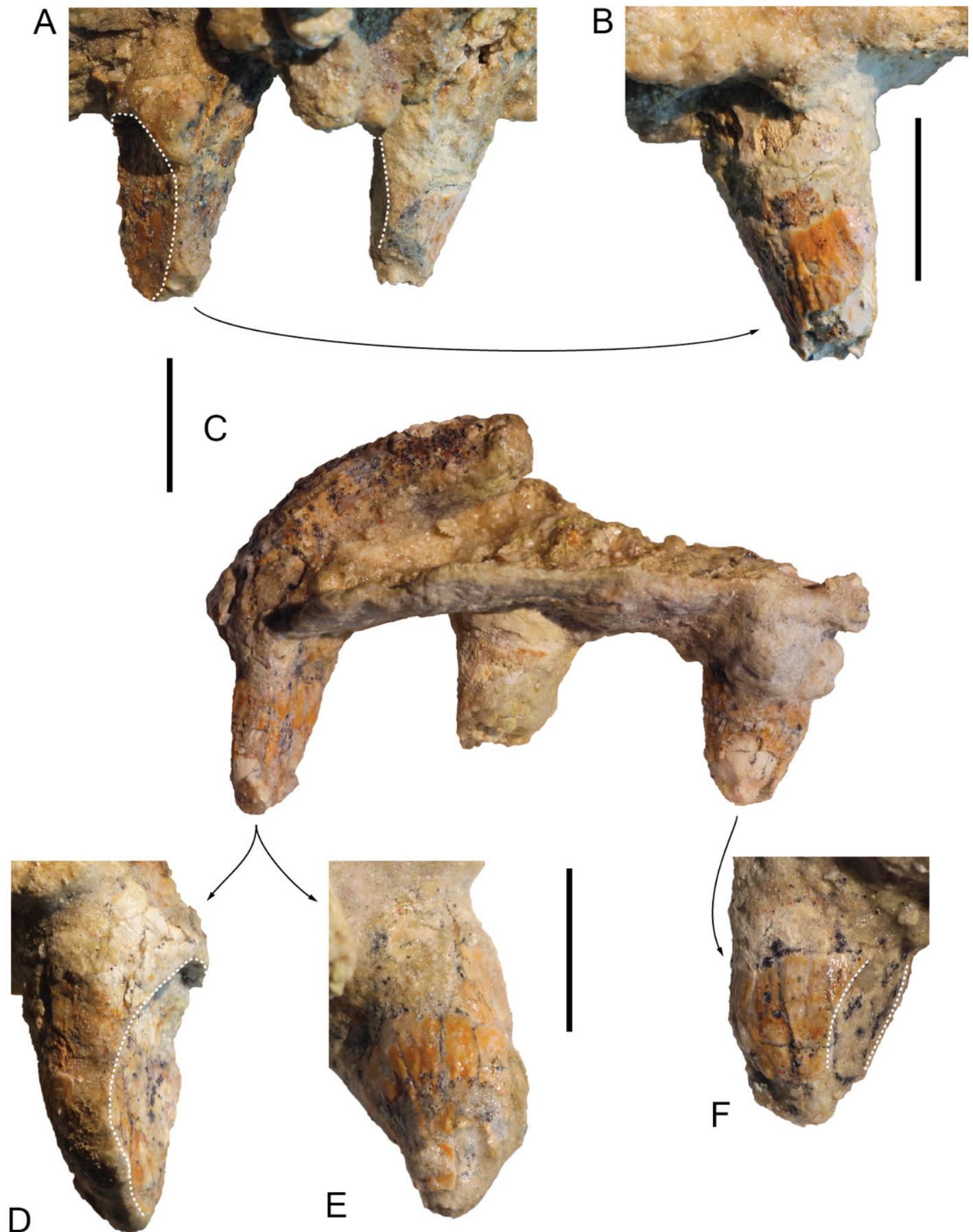


Figure 12

Cervical vertebrae of *Kwanzacetes adamsi*.

A-D, axis of the holotype of *K. adamsi* CZA 4 in anterior (A), left lateral (B), posterior (C), and ventral (D) views; E-F, cervical ?C3-C4 CZA 5 in anterior (E) and right lateral (F) views. Scale bar equals 50 mm.

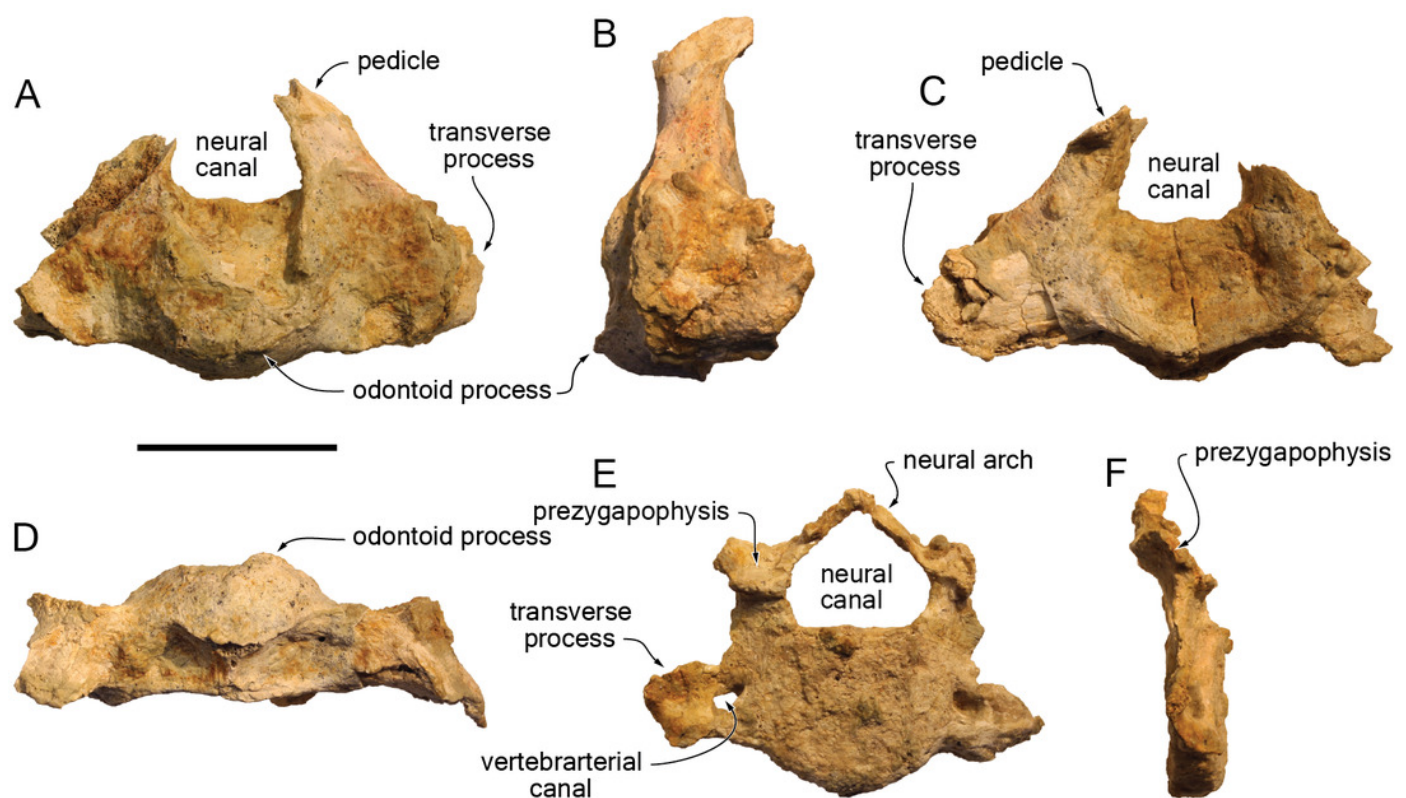


Figure 13

Phylogenetic relationships of *Kwanzacetus adamsi*.

Phylogenetic tree showing the relationships of *K. adamsi* with other early diverging delphinidans, as obtained from our parsimony analysis of morphological data, constrained with a molecular tree as backbone. Other odontocete clades are collapsed to facilitate reading. *K. adamsi* falls as an iniid, displaying close relationships with the extant *Inia geoffrensis*. Stars identify species with a strictly freshwater distribution (or, in the case of *Platanista gangetica*, the superfamily Platanistoidea to whom it belongs).

